

Electric Vehicle Routing Problem with Flexible Deliveries

Mir Ehsan Hesam Sadati^{a,b}, Vahid Akbari^c, Bülent Çatay^{a,b,*}

^a Faculty of Engineering and Natural Sciences, Sabanci University, Istanbul, Turkey

^b Smart Mobility and Logistics Lab, Sabanci University, Istanbul, Turkey

^c Nottingham University Business School, University of Nottingham, Jubilee Campus,
Nottingham NG8 1BB, United Kingdom

Abstract: In the past few years, growing concerns about the climate change have forced governments to initiate tighter environmental regulations and tougher emission reduction targets. These initiatives have increased the interest on alternative fuels and heightened the public awareness on electromobility. To cut their dependency on fossil fuels, logistics operators started employing electric vehicles (EVs) in their fleet, which brings in additional challenges to their operational planning. In addition, with an ever-growing interest in e-commerce, parcel delivery is taking new shapes by offering flexible delivery options to the customers. To mitigate these issues, we introduce the Electric Vehicle Routing Problem with Flexible Deliveries (EVRP-FD), where the customers are served using a fleet of EVs that can recharge their batteries along their routes. In this problem, a customer may specify multiple delivery locations and the delivery can be made to one of these locations within its predetermined time window. Our objective is to minimize the total distance travelled by using minimum number of vehicles in the fleet. We first formulate the mathematical model of the problem. Next, we develop a hybrid Variable Neighborhood Search method coupled with Tabu Search by proposing new mechanisms to solve the problem effectively. Then, we verify the performance of our algorithm on instances published in the literature. We also introduce new instances for the EVRP-FD and perform an extensive computational study to investigate the trade-offs associated with different operational factors. Finally, we present a case study in Nottingham, UK to provide further insights.

Keywords: Electric vehicle routing problem, flexible deliveries, variable neighborhood search, granular tabu search, recharging.

* Corresponding author. Email: catay@sabanciuniv.edu

1. Introduction

The rapid development of e-commerce in recent years stimulates the growth of the logistics industry. In 2018, nearly 3 billion people enjoyed online shopping at least once. Furthermore, the turnover from e-commerce was estimated to be around 2875 billion dollars, with a growth of 12% compared to its previous year (Marco et al., 2020). Online shopping has shown a tremendous growth in 2020 globally because of the COVID-19 pandemic. Consumers are likely to continue their online consumption habits in the future (UNCTAD, 2020). The significant rise in e-commerce results in a considerable challenge in the “last-mile” of the supply chain, which is the final delivery of the goods to the consumers. These last-mile challenges are aggravated considering new flexibilities that logistic companies are offering to their customers. For example, DHL defines *logsumers* as customers who can individualize their orders by choosing multiple delivery options and time windows based on their availability at different locations (Bubner et al., 2014). UPS initiated the *Alternate Delivery Program* in which the package can be delivered to a designated UPS location or a participating neighborhood store (e.g. a deli, dry cleaner, coffee shop) rather than to the recipient’s primary residence or place of business. Then, the customers can pick up their parcels at their convenience (ups.com). In a similar setting, the customers may request their packages to be delivered into the trunk of their cars parked at pre-specified locations (Reyes et al., 2017). On the one hand, logistics companies are encouraged to offer such flexibilities in their last-mile services together with faster deliveries. On the other hand, environmental concerns regarding congestion, noise and air pollution force them to invest in efficient and clean last-mile delivery systems.

The majority of the logistics operators mostly utilize diesel-powered vehicles in their delivery services (Lewis et al., 2020). However, due to the negative externalities caused by internal combustion engine vehicles (ICEVs) such as carbon emissions, air pollution, and climate change, governments and city municipalities impose more strict regulations to freight transportation with these vehicles in cities (Pan et al., 2021b). The European Commission coordinated actions to achieve CO₂-free urban logistics in major city centers by 2030 (European Commission, 2013). The Netherlands and Norway stepped up measures to phase out ICEVs by 2025 and German Federal Council passed a resolution that bans the sale of ICEVs from 2030 onward (fuelsave-global.com). Recently, UK also declared that the sale of new diesel- and petrol-powered vans and cars would

be banned from 2030 (bbc.com). Furthermore, President Joe Biden signed an executive order for converting the U.S. government's fleets, including 225,000 Postal Service vehicles, to electric vehicles (reuters.com). These initiatives encourage the shift towards alternative fuel vehicles (AFVs), mainly electric vehicles (EVs), for both private and commercial uses. Consequently, battery electric vehicles (BEVs) are expected to constitute a large share within the fleets of logistics operators. In 2019, Amazon co-founded the Climate Pledge and committed to purchase 100,000 electric delivery vehicles to zero down their carbon emissions by 2040. The company's EVs have recently started making deliveries in Los Angeles, with an expansion plan across 15 additional cities in 2021 (businessinsider.com).

BEVs are vehicles that are entirely powered by a rechargeable battery. They have zero tailpipe emission and are categorized as the cleanest vehicles in transportation (Jaller et al. 2018). The structure of the BEVs is simpler than other EV types (EVs) as it uses mono-power from the battery, removes the combustion engine, transmission, fuel tank, cooling, and exhaust system. Thus, its maintenance service is relatively simpler and cheaper. However, the limited driving range, high battery cost, long recharging times, and limited recharging facility infrastructure remain the main drawbacks of the BEVs (Giordano et al., 2017). These limitations bring in additional complexities for logistics operators in their fleet management and route planning. Hence, the arising optimization problems have attracted considerable attention in the Vehicle Routing Problem (VRP) literature, and various variants of the Electric Vehicle Routing Problem (EVRP) have been introduced and studied over the past decade. In this study, we attack the Electric Vehicle Routing Problem with Flexible Deliveries (EVRP-FD), where the customers have the flexibility to request their orders to be delivered to one of the alternative delivery locations within the predetermined time windows. To the best of our knowledge, this particular problem has not been studied in the literature.

In the EVRP-FD, a homogenous fleet of commercial (battery) EVs are dispatched from a single depot. For consistency with the terminology established in the literature, we use the term EV referring to a BEV in the rest of the article. The customers are allowed to specify alternative delivery locations and time windows for their orders, and the order is delivered to exactly one of these locations within the corresponding time window. Since the EVs have limited autonomy, they may need to recharge their batteries en-route in order to continue their tour. Our objective is to minimize the total distance travelled by using minimum number of vehicles in the fleet. We first

present the 0-1 mixed integer linear programming (MILP) model of the problem. Since the problem is not tractable for large-size instances, we develop a Variable Neighborhood Search (VNS) method that benefits from Tabu Search (TS) in local search. To reduce the computational effort, we use Granular TS approach (Toth and Vigo, 2003). Hence, the proposed algorithm is referred to as the Variable Neighborhood Search/Granular Tabu Search (VNS/GTS). In both shaking and local search phases, we employ several problem-specific neighborhood structures. We present an extensive experimental study to investigate the performance of the proposed method and provide insights for both researchers and practitioners.

Our contributions can be summarized as follows: (i) we introduce the EVRP-FD and formulate its MILP model; (ii) we develop a hybrid VNS and TS method by proposing several new problem-specific neighborhood structures; (iii) we introduce new benchmark instances for the EVRP-FD and perform extensive computational experiments to assess the performance of the proposed method; (iv) we present various trade-off analyses concerning key parameters and provide managerial insights; (v) we conduct a case study based on data collected from Nottingham, UK.

The rest of the paper is structured as follows: In Section 2 we review the relevant literature. In Section 3, we describe the EVRP-FD and introduce its mathematical model. The proposed VNS/GTS method is presented in Section 4. Section 5 details the experimental study and discusses the results. Section 6 presents the case study while Section 7 concludes the paper with final remarks and future research directions.

2. Literature review

The delivery flexibility was first considered by de Jong et al. (1996) within the context of VRP with Multiple Time Windows (VRPMTW). Doerner et al. (2008), Favaretto et al. (2013), Belhaiza et al. (2014), and Beheshti et al. (2015) also addressed VRPMTW; however, none of these studies allowed customers to select alternative locations for their deliveries. Another vein of literature that incorporated flexibility in delivery is the Generalized VRP (GenVRP) introduced in Ghiani and Improta (2000). In the GenVRP, customers are grouped into clusters, and it is sufficient if a delivery vehicle visits one of the nodes within each cluster. Different from our problem in which customers have multiple delivery locations in different time windows, in the GenVRP, multiple customers are served by a single visit to the cluster at any time.

Reyes et al. (2017) extended the VRPMTW to the Vehicle Routing Problem with Roaming Delivery Locations (VRPRDL), where a good may be delivered into the trunk of the customer's car during different time slots throughout the day if the customer is not available for a direct pickup at home. In other words, the customer may have multiple delivery options at different time intervals. For each of these delivery options, the time windows were assumed to be non-overlapping. The authors proposed construction and improvement heuristics to solve the VRPRDL. Although the VRPRDL does not involve the routing of electric vehicles, it has some similarities with our problem with respect to other characteristics. Ozbaygin et al. (2017) also tackled the VRPRDL and developed a branch-and-price algorithm to solve it. Using their branch-and-price algorithm, they also solved a hybrid variation of the VRPRDL in which home delivery is possible at any time during the planning horizon. Ozbaygin et al. (2019) addressed the dynamic variant of the VRPRDL where delivery plans may change during the execution of a planned schedule. Because of the changes, the planned schedule may become sub-optimal or infeasible. So, the authors proposed a branch-and-price algorithm to re-optimize the vehicle routes and delivery locations.

Very recently, Tilk et al. (2021) studied another variant of the VRPRDL in which the goods may be delivered to shared locations such as shops and parcel lockers instead of the trunk of the cars and shared delivery locations are associated with service capacities. One drawback in this setting is that each shared location is associated with a common time window; hence, many deliveries to that location may take place earlier than their actual time windows, which may lead to inefficient utilization of vehicle as well as location capacities. In a different business model, Pan et al. (2021a) used parcel lockers for transferring goods/items between EVs, vans, and bikes within the context of Multi-Depot VRP in an attempt to enhance the capability and sustainability of dispatcher networks.

To the best of our knowledge, Conrad and Figliozzi (2011) is the first study that addressed the VRP using a fleet of EVs and referred to the problem as the Recharging VRP (RVRP). In this problem, the EVs are allowed to recharge at selected customers locations either to full or to 80% battery capacity. The recharge duration is assumed constant. Erdoğan and Miller-Hooks (2012) generalized this problem and introduced the Green VRP (GVRP) where the fleet consisted of AFVs. AFVs can refuel en-route at alternative fueling stations (AFSs) where the fuel tank is filled to full capacity in constant time. Schneider et al. (2014) extended it to the Electric Vehicle Routing

Problem with Time-Windows (EVRPTW) by also assuming that the EVs are fully charged at recharging stations. However, the recharging time is assumed proportional to the energy transferred and depends on the battery state of charge (SoC) when the EV arrives at the station. The authors adopted a hierarchical objective function that minimizes the number of vehicles first and the total distance traveled second, and implemented three different approaches based on VNS and TS.

The full recharge restriction was relaxed by Bruglieri et al. (2015) and Keskin and Çatay (2016) who allowed partial recharges. Keskin and Çatay (2016) extended the model of Schneider et al. (2014) and developed an ALNS approach to solve it. Bruglieri et al. (2015) considered an objective function that includes the travel time, waiting time, recharging time as well as the number of vehicles, and used a VNS Branching method to solve small-size instances. Desaulniers et al. (2016) studied the EVRPTW with both full and partial recharging cases, and attempted to solve those optimally using branch-price-and-cut algorithms. Recently, Duman et al. (2021) developed exact and heuristic methods based on branch-and-price-and-cut to solve the same problem, and presented new best solutions. Cortés-Murcia et al. (2019) extended the EVRPTW where the customer can be served via alternative transportation methods (walking, bikes, drones, etc.) while the EV is being recharged at the station. The authors developed an Iterated Local Search (ILS) method and investigated the financial benefits of serving customers while charging.

Several studies addressed various EVRP extensions with regard to battery charging and discharging rates including rapid charging (Felipe et al., 2014; Çatay and Keskin, 2017; Keskin and Çatay, 2018), more accurate energy consumption estimation considering external and internal factors (Goeke and Schneider, 2015; Rastani et al., 2019; Kancharla and Ramadurai, 2020; Rastani et al., 2020; Rastani and Çatay, 2021), and non-linear charging function (Montoya et al., 2017; Froger et al., 2019; Kancharla and Ramadurai, 2020). Other extensions include the availability of stations and stochastic recharging times (Sweda et al., 2017; Keskin et al., 2019; Kullman et al., 2019; Keskin et al., 2021), fleet composition (Goeke and Schneider, 2015; Hiermann et al., 2016; Mancini, 2017; Sassi and Oulamara, 2017; Macrina et al., 2019; Hiermann et al., 2019), battery swapping (Yang et al., 2015, Hof et al., 2017; Wang et al., 2018; Masmoudi et al., 2019; Jie et al., 2019), and the utilization of hybrid electric vehicles (Zhen et al., 2015). We refer the reader to Erdelić and Carić (2019) for an extensive review about the utilization of EVs in goods distribution.

3. Problem description and mathematical formulation

EVRP-FD deals with a homogenous fleet of EVs serving customers with known demands and alternative delivery points and time windows. The good is delivered to one of these locations within the desired time window. The EVs have limited driving range because of the battery energy capacity and may need to recharge en-route in order to continue their tours. Discharging the battery completely and recharging it to full capacity shortens its lifespan and can take hours (Sweda et al., 2017). As Pelletier et al. (2017) highlighted logistics companies often operate within 10-20% to 80-90% range of battery capacity, which corresponds to the first phase of recharging where the charge duration is a linear function of the amount of energy transferred. Therefore, without loss of generality we assume that EVs are operated between 10% and 90% of their battery capacity. Furthermore, we allow EVs to recharge only at the company-owned depot, which is the practical case in real-world logistics operations considering the limited recharging infrastructure in most regions. Even though numerous public recharging stations may exist in the region, not all of them will be truck friendly (Baker et al., 2016). In addition, due to the other factors including inefficient use of drivers' time and security concerns related to the cargo onboard many companies using EVs prefer recharging the vehicles at their own facilities (Morganti and Browne, 2018). Note that public recharging stations can be easily incorporated in our solution methodology and we present a detailed numerical analysis of this case in our experimental study.

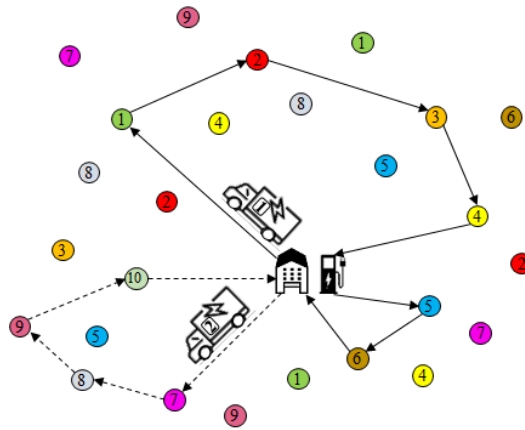


Fig. 1. An illustrative example

Fig. 1 provides an illustrative example that involves 10 customers with 26 delivery locations in total. The node numbers represent the customers. The nodes with the same ID number represent the alternative delivery locations of a customer. For instance, customer C1 has three alternative locations shown as nodes numbered “1” and highlighted in green. In this example, EV#1 departs from the depot, visits customers C1 thru C4, and returns to depot for recharging. After recharging, it continues its route by visiting customers C5 and C6, and then returns to depot at the end of its tour. EV#2 departs from the depot, serves customers C7 thru C10, completes its tour and returns to depot without recharging.

In the following, we provide the mathematical notation and formulation of the EVRP-FD. Let V^c denote the set of all customers and L^c for $c \in V^c$ denote the set of locations selected by customer c . Let V be the set of all the locations ($V = \bigcup_{c \in V^c} L^c$). We denote the depot by 0 and $n + 1$ at the beginning and end of a route, respectively. Then, we define sets $V_0 = V \cup \{0\}$, $V_{n+1} = V \cup \{n + 1\}$, and $V_{0,n+1} = V \cup \{0, n + 1\}$. Each node $i \in V_{0,n+1}$ is associated with time window $[e_i, l_i]$. The service time at each node is represented by $s_i, i \in V$. The recharging rate is denoted by g and the cargo capacity of the vehicle is C . The parameters d_{ij} , t_{ij} , and h_{ij} represent the distance, travel time, and energy consumption from node $i \in V_0$ to node $j \in V_{n+1}$, respectively.

Similar to the approach of Bruglieri et al. (2016), we define d'_{ij} , t'_{ij} , and h'_{ij} to denote the additional (detouring) distance, travel time and energy consumption, respectively, associated with visiting the recharging station on the trip from i to j as follows: $d'_{ij} = d_{i0} + d_{0j} - d_{ij}$, $t'_{ij} = t_{i0} + t_{0j} - t_{ij}$, and $h'_{ij} = h_{0i} + h_{0j} - h_{ij}$. Binary variable x_{ij} is equal to 1 if an EV travels from node i to node j ; 0 otherwise; and z_{ij} is equal to 1 if a vehicle recharges on its trip from node i to node j ; 0 otherwise. We keep track of the battery state of charge (SoC) in terms of the fraction of the battery capacity. The continuous decision variables y_i and r_i denote the battery SoC when the EV arrives at node i and the amount of energy recharged on its way to node i , respectively. τ_i indicates the service start time at node i and u_i shows the remaining cargo on the vehicle upon arrival to node i . The mathematical notation is summarized in Table 1.

Table 1. Mathematical notation**Sets:**

V	Set of all locations
V^c	Set of customers
L^c	Set of locations of customer $c \in V^c$
V_0	Set of locations and the depot, $V_0 = V \cup \{0\}$
V_{n+1}	Set of locations and the sink node, $V_{n+1} = V \cup \{n + 1\}$
$V_{0,n+1}$	Set of locations, the depot and the sink node, $V_{0,n+1} = V \cup \{0, n + 1\}$

Parameters:

t_{ij}	Travel time from node i to node j
t'_{ij}	Detouring time to visit the recharging station on the trip from node i to node j , $t'_{ij} = t_{i0} + t_{0j} - t_{ij}$
d_{ij}	Distance from node i to node j
d'_{ij}	Detouring distance to visit the recharging station on the trip from node i to node j , $d'_{ij} = d_{i0} + d_{0j} - d_{ij}$
h_{ij}	Energy consumed to traverse arc (i, j)
h'_{ij}	Energy consumed for detouring to visit the recharging station on the trip from node i to node j , $h'_{ij} = h_{i0} + h_{0j} - h_{ij}$
$[e_i, l_i]$	Time window associated with node i
s_i	Service time at node i
F	A sufficiently large constant
C	Cargo capacity of the vehicle
g	Recharging rate of the charger

Decision variables:

x_{ij}	1 if arc (i, j) is traversed by a vehicle; 0 otherwise
z_{ij}	1 if a vehicle recharges on the trip from node i to node j ; 0 otherwise
r_i	Amount of energy recharged when a vehicle travels to node i , $0 \leq r_i \leq 1$
τ_i	Service start time of node i by one of the vehicles
y_i	Battery SoC at node i , $0 \leq y_i \leq 1$
u_i	Load on the vehicle upon its arrival at node i

Then, the EVRP-FD can be formulated as a MILP model as follows:

$$\min \left(\sum_{j \in V_{n+1} \setminus \{i\}} \sum_{i \in V_0} d_{ij} x_{ij} + \sum_{j \in V \setminus \{i\}} \sum_{i \in V} d'_{ij} z_{ij} \right) + F \left(\sum_{i \in V} x_{0i} \right) \quad (1)$$

subject to:

$$\sum_{i \in L^c} \sum_{j \in V_{n+1} \setminus \{i\}} x_{ij} = 1 \quad c \in V^c \quad (2)$$

$$\sum_{j \in V_0, j \neq i} x_{ji} = \sum_{j \in V_{n+1}, j \neq i} x_{ij} \quad i \in V \quad (3)$$

$$z_{ij} \leq x_{ij} \quad i \in V, j \in V \setminus \{i\} \quad (4)$$

$$r_j \leq \sum_{i \in V, i \neq j} z_{ij} \quad j \in V \quad (5)$$

$$\tau_i + (t_{ij} + s_i) + t'_{ij} z_{ij} + g \times r_j - l_0(1 - x_{ij}) \leq \tau_j \quad i \in V_0, j \in V_{n+1} \setminus \{i\} \quad (6)$$

$$e_i \leq \tau_i \leq l_i \quad i \in V_{0,n+1} \quad (7)$$

$$0 \leq u_j \leq u_i - q_i x_{ij} + C(1 - x_{ij}) \quad i \in V_0, j \in V_{n+1} \setminus \{i\} \quad (8)$$

$$0 \leq u_0 \leq C \quad (9)$$

$$y_j \leq y_i - h_{ij} - h'_{ij} z_{ij} + r_j + (1 - x_{ij}) \quad i \in V_0, j \in V_{n+1} \setminus \{i\} \quad (10)$$

$$y_0 = 1 \quad (11)$$

$$y_i \geq h_{i0} \sum_{j \in V \setminus \{i\}} z_{ij} \quad i \in V \quad (12)$$

$$0 \leq y_j \leq (1 - h_{0j}) + (1 - \sum_{i \in V \setminus \{j\}} z_{ij}) \quad j \in V \quad (13)$$

$$0 \leq r_j \leq 1 - (y_i - h_{i0}) + (1 - z_{ij}) \quad i \in V, j \in V \setminus \{i\} \quad (14)$$

$$x_{ij} \in \{0,1\} \quad i \in V_0, j \in V_{n+1} \setminus \{i\} \quad (15)$$

$$z_{ij} \in \{0,1\} \quad i \in V, j \in V \setminus \{i\} \quad (16)$$

The objective function (1) minimizes the total distance traveled by utilizing minimum number of EVs. The latter is achieved with the second term by using a sufficiently large constant F that represents a fixed cost for the vehicles. Constraints (2)–(3) are the flow balance constraints that guarantee that each customer is visited exactly once at one of its predetermined locations. Constraints (4) ensure that if an EV recharges its battery on the trip from node i to node j then it serves node j after node i . Constraints (5) allow a positive recharge amount only if the EV recharges its battery on its trip from all other nodes to node j . Constraints (6) keep track of the time at customers (and the depot) while constraints (7) establish the service time window restrictions. Constraints (8) and (9) ensure that vehicle capacities are not exceeded. Constraints (6)–(9) also prevent the formation of subtours. Constraints (10) keep track of the battery SoC at customers (and

the depot) and constraints (11) set the SoC of the EVs to full upon their departure from the depot. Constraints (12) guarantee that the EV has sufficient energy to reach the station if it recharges its battery on the trip from node i to node j . Constraints (13) ensure that the battery is never recharged beyond its capacity while constraints (14) make sure the amount of energy recharged does not exceed the remaining capacity of the battery. Finally, constraints (15) and (16) define the domain of the binary variables

4. Solution methodology

In our VNS/GTS the neighborhood structures are systematically changed in the shaking phase of the general VNS scheme (Mladenović and Hansen, 1997) and the Granular Tabu Search (GTS) algorithm (Toth and Vigo, 2003) is implemented as the local search method. VNS is one of the most successful heuristic algorithms for solving hard combinatorial optimization problems despite its simple algorithmic structure requiring few parameters. It has been successfully applied to various routing problems such as the EVRPTW (Schneider et al. 2014), VRP with two-dimensional loading constraints (Wei et al., 2015), battery swap station location-routing problem (Hof et al., 2017), clustered VRP (Hintsch and Irnich 2018), Dial-a-Ride Problem with EVs (Masmoudi et al., 2018), single VRP with deliveries and selective pickups (Coelho et al., 2016), profitable heterogeneous VRP with cross-docking (Baniamerian et al., 2019), fleet size and mix VRP with electric modular vehicles (Rezgui et al., 2019), and the double VRP with multiple stacks (Chagas et al., 2020).

The recent literature has shown that combining two or more metaheuristic algorithms can enhance the performance of the algorithms in terms of the computation time and/or solution quality (Ting et al., 2015). VNS has been hybridized with different approaches for solving many combinatorial optimization problems including Genetic Algorithm (Paydar et al., 2013, Xia et al., 2016, Li et al., 2018), Simulated Annealing (Abbasi et al., 2011, Hosseini et al., 2014), Particle Swarm Optimization (Marinakos et al. 2017) as well as Integer Linear Programming (Prandtstetter and Raidl, 2008). VNS with TS combination was also used to solve VRP variants such as VRP with clustered backhauls and 3D loading constraints (Bortfeldt et al., 2015), VRP with drones and en-route operations (Schermer et al., 2019), multi-depot VRP (Sadati et al., 2020; Sadati et al., 2021), and multi-depot green VRP (Sadati and Çatay, 2021). A recent taxonomic review of Elshaer and

Awad (2020) indicates that VNS and TS are the two most frequently utilized algorithms in solving the VRP and its variants. These successful implementations constitute our main motivation in coupling VNS with GTS in this study.

Algorithm 1. The pseudocode of VNS/GTS	
<i>Notation:</i>	
S_0 :	Initial solution
S_{GTS} :	Solution produced by Granular Tabu Search
\bar{S} :	Current solution
S^* :	Incumbent solution
$Z(S)$:	Objective function value of solution S
$N_k(S)$:	k^{th} neighborhood of solution S
1:	Construct S_0 <i>// Construct initial solution</i>
2:	Set $\bar{S} = S^* = S_0$ and $Z(\bar{S}) = Z(S_0) = Z(S^*)$
3:	Repeat
4:	For $k = 1$ to k_{max} do
5:	Generate random solution S' using $N_k(\bar{S})$ <i>// Shaking</i>
6:	Apply Granular Tabu Search to obtain S_{GTS} <i>// Local Search</i>
7:	Set $\bar{S} = S_{GTS}$
8:	If \bar{S} is feasible and $Z(\bar{S}) < Z(S^*)$
9:	Update $S^* = \bar{S}$
10:	Set $k = 1$
11:	Else
12:	Set $k = k + 1$
13:	End If
14:	End For
15:	Set $\bar{S} = S^*$
16:	Until Stopping Condition

VNS/GTS starts with an initial solution S_0 constructed using the greedy insertion algorithm. Initially, the current solution \bar{S} and the incumbent solution S^* are set to $\bar{S} = S^* = S_0$. Then, the shaking phase is implemented using a set of neighborhood structures N_k ($k = 1, \dots, k_{max}$). In this phase, a random solution S' is generated by applying the first neighborhood operator N_1 to solution \bar{S} . Next, GTS is performed in the local search phase by applying a pre-determined set of neighborhood operators to obtain a new solution S_{GTS} . We then set the current solution $\bar{S} = S_{GTS}$. If \bar{S} is feasible and improves the incumbent solution S^* , then S^* is replaced with \bar{S} and the neighborhood counter k is reset to 1 (i.e., we return to the first shaking neighborhood structure).

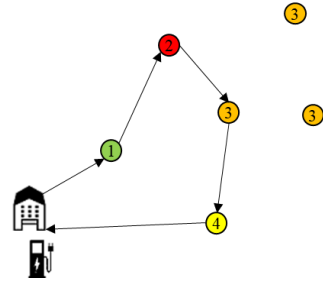
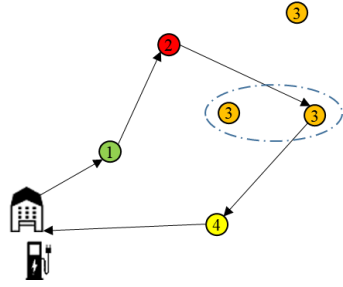
Otherwise, k is increased by 1 ($k = k + 1$) and VNS/GTS continues by applying another shaking move on \bar{S} . In the subsequent iteration of shaking solution \bar{S} will be considered, regardless of whether it is feasible or not. If all neighborhood structures are explored ($k = k_{max}$), the algorithm restarts from the best solution found so far S^* and neighborhood structure index k is re-initialized to 1. This procedure is repeated until a termination condition is satisfied. The algorithm terminates if the solution is not improved for a pre-determined number of iterations ($Iter_{NonImp}$) or reaches a pre-determined number of iterations ($Iter_{Total}$). The pseudocode of the VNS/GTS is presented in Algorithm 1.

4.1. Initial solution construction

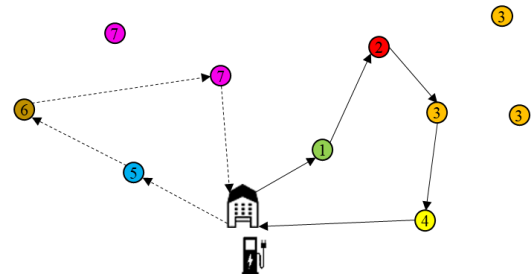
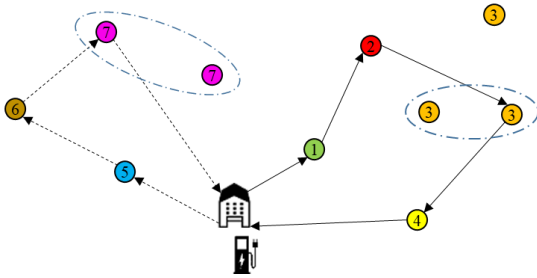
To construct an initial feasible solution for the EVRP-FD we apply a greedy insertion heuristic. First, we determine the nearest delivery location of each customer to the depot. Among them, the farthest location is selected and the route is initialized by serving the corresponding customer at the selected location and returning to the depot. Then, the cheapest insertion rule is used to add the remaining customers to the route. For all unvisited customers, we consider all their alternative delivery locations, determine the feasible location and position pair that increases the objective function value the least, and perform the insertion. If we cannot insert any customers feasibly, then we close the current route and initialize a new route. We repeat this procedure until all customers have been served.

4.2. Shaking

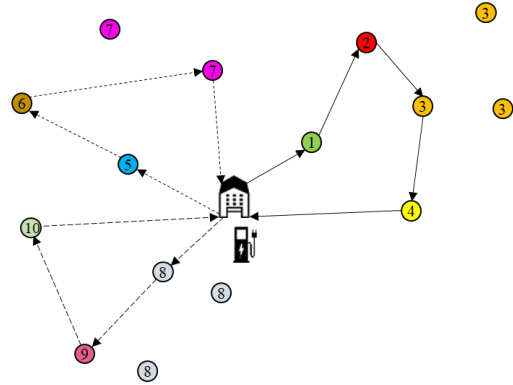
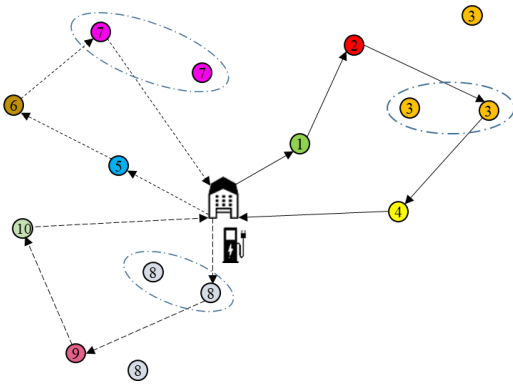
In the shaking phase of VNS/GTS, a random solution is constructed using three types of problem-specific neighborhood structures: λ -*SwitchLocation*, κ -*MoveCustomer*, and *Merge*. The λ -*SwitchLocation* neighborhood operator switches the delivery location of λ customers with their alternative delivery locations in λ routes (one switch in each selected route). If a customer has two or more alternative delivery locations, one is selected randomly. In this study, we use three types of λ -*SwitchLocation* moves and refer to them as 1-*SwitchLocation*, 2-*SwitchLocation*, and 3-*SwitchLocation*. These moves are illustrated in Fig. 2.



(a) 1-SwitchLocation operator



(b) 2-SwitchLocation operator



(c) 3-SwitchLocation operator

Fig. 2. λ -SwitchLocation shaking operators

The κ -MoveCustomer is applied to the routes of two vehicles. In this neighborhood structure, the first κ customers from the second route are removed and appended to the end of the first route by inserting a recharge visit. Since the first route will start by serving κ more customers, this operator may cause time-window violations for the customers moved. However, we observed that it may help the algorithm reach an improved feasible solution in the subsequent local search phase or in

the following iterations. We employ *1-MoveCustomer*, *2-MoveCustomer* and *3-MoveCustomer* in our implementation as shown in Fig. 3.

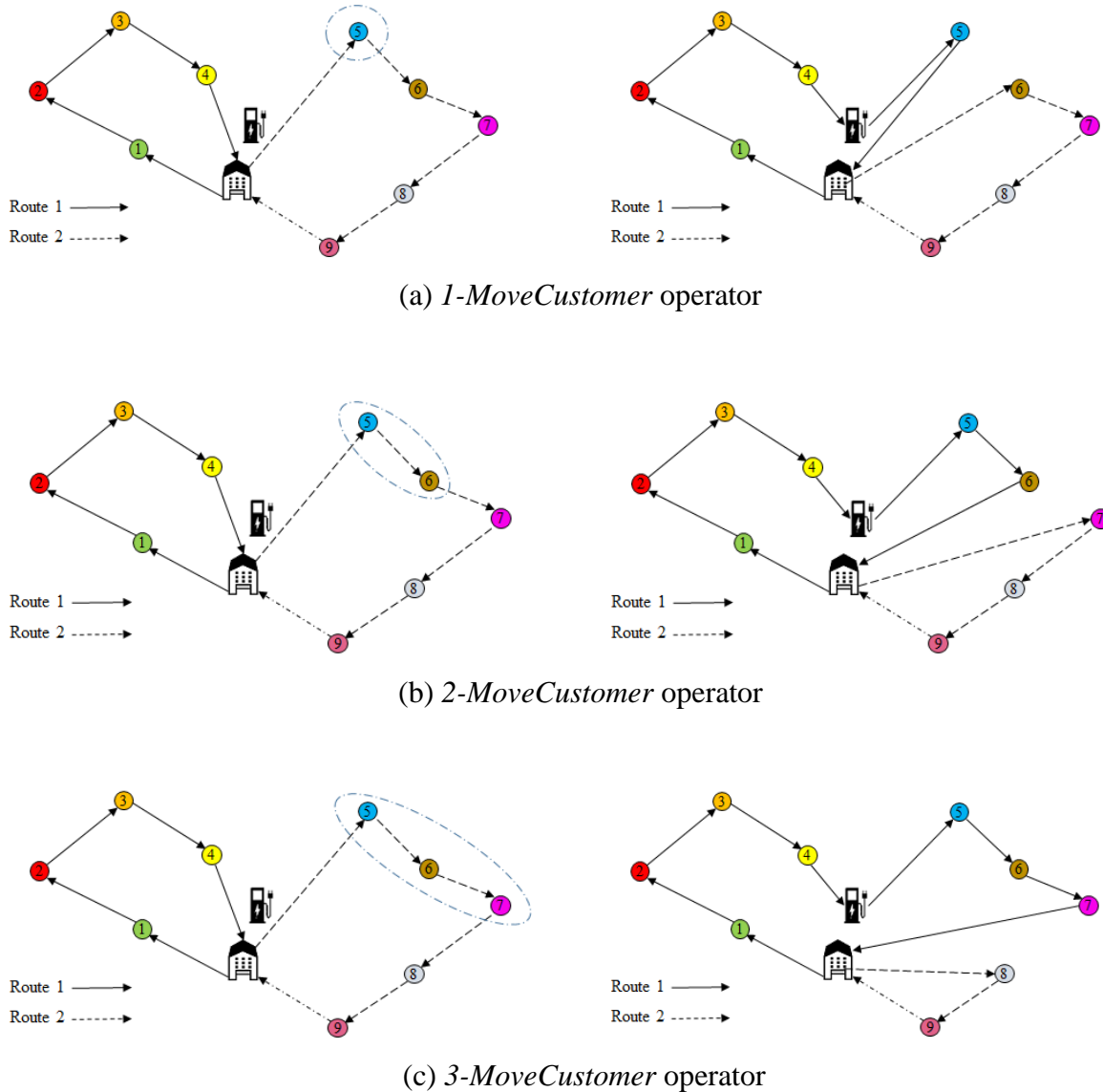


Fig. 3. κ -*MoveCustomer* shaking operators

The Merge move merges two routes by appending one to the end of the other while keeping the direction of the journey. It is implemented in two ways by traveling from the last location in the first route to the first location in the second route directly (Fig. 4.a) or via recharging station (Fig.

4.b). This operator aims at reducing the fleet size but it also helps decreasing the total distance traveled according to the triangular inequality property. On the other hand, the resulting merged route can be infeasible with respect to the driving range and time window constraints, and similar to previous neighborhood operator this infeasibility may allow the algorithm reach an improved feasible solution in the subsequent local search phase. All neighborhood structures of the shaking phase are investigated in cyclic order starting from 1-SwitchLocation and ending with Merge.

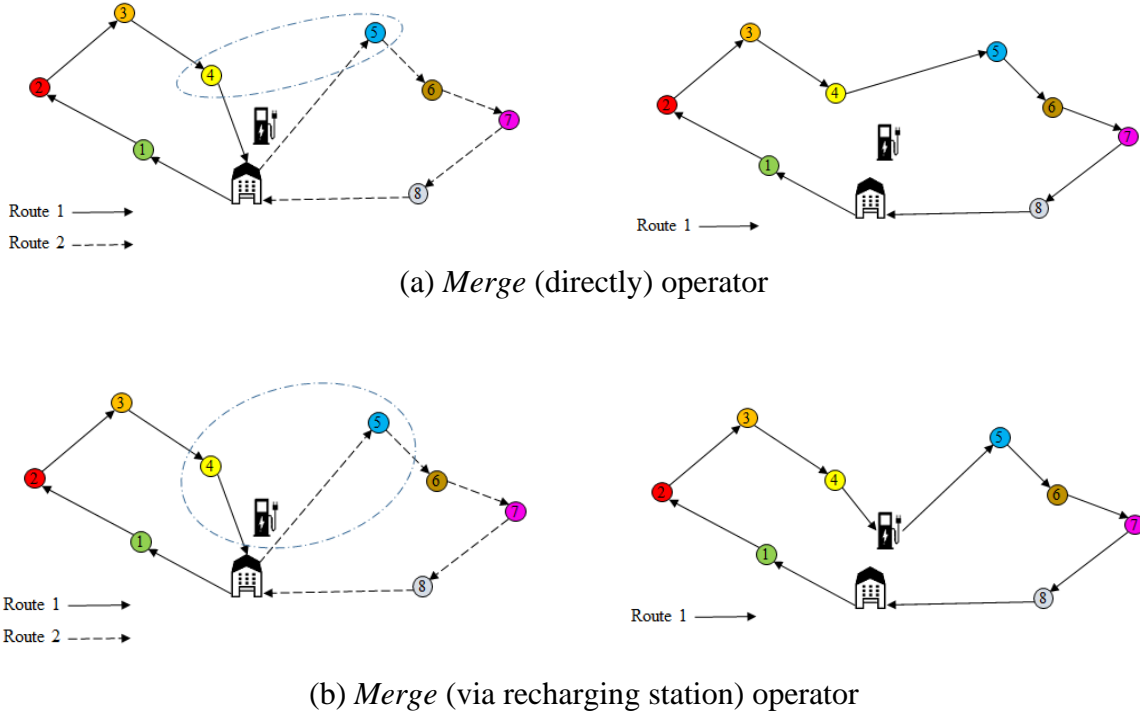


Fig. 4. Merge shaking operators

4.3. Strategic oscillation for handling infeasible solutions

VNS/GTS is equipped with strategic oscillation for allowing infeasible solutions (Cordeau et al., 1997). If a neighborhood operator fails to generate a feasible solution, this infeasible solution is accepted by penalizing its objective function value using a multiplier proportional to the amount of infeasibility as follows:

$$Z'(S) = Z(S) + \alpha D(S) + \beta W(S) + \gamma C(S) \quad (17)$$

where

$$D(S) = \sum_{i \in V_0} \sum_{j \in \{V_{n+1} \setminus i\}} [y_j - y_i + h_{ij} + h'_{ij} z_{ij} - r_j - (1 - x_{ij})]^+ \quad (18)$$

$$W(S) = \sum_{i \in V_0} [\tau_i - l_i]^+ \quad (19)$$

$$C(S) = \sum_{i \in V_0} \sum_{j \in \{V_{n+1} \setminus i\}} [u_j - u_i + q_i x_{ij} - C(1 - x_{ij})]^+ \quad (20)$$

In Equation (17), $Z(S)$ refers to the objective function value defined in (1) which is associated with solution S , and $D(S)$, $W(S)$ and $C(S)$ indicate the violations in driving range, time windows and vehicle cargo capacity, respectively. Note that $[\blacksquare]^+ = \max\{0, \blacksquare\}$. The parameters α , β , and γ are positive constants to penalize the infeasibilities $D(S)$, $W(S)$, and $C(S)$, respectively. We update the penalty parameters at each iteration of the GTS to obtain feasible and infeasible solutions with approximately the same frequency. If the driving range of a solution S is feasible, then its corresponding penalty parameter will be updated as $\alpha = \alpha / (1 + \delta)$; otherwise, it will be updated as $\alpha = \alpha(1 + \delta)$. The same procedure is employed to β and γ as well. The δ is the parameter used to update α , β , and γ .

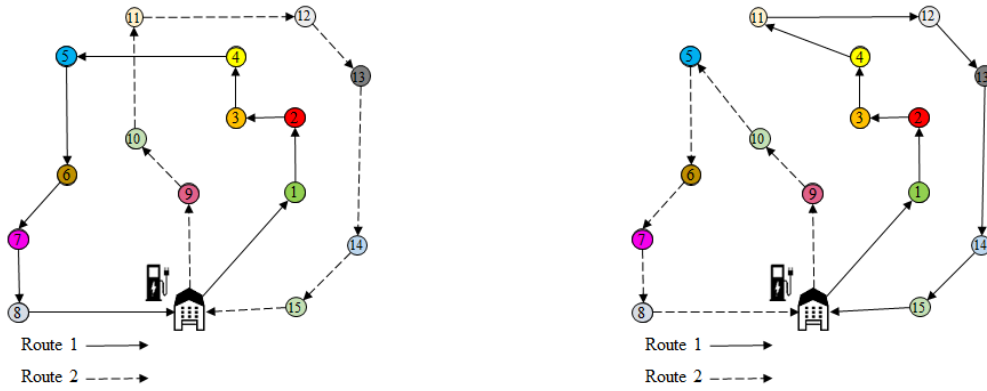
4.4. Granular tabu search

After shaking the solution, TS is employed in an attempt to improve the current best (incumbent) solution using five neighborhood operators. Since evaluating all possible neighborhoods may be computationally expensive, we employ the granular search approach of Toth and Vigo (2003) to reduce the run time. Each neighborhood is associated with a tabu condition that prevents returning to the previously explored solutions. For each neighborhood, we revoke the tabu condition at the end of the tabu duration η or if the aspiration criterion is met, i.e. if a new best solution is obtained. GTS is performed for a pre-determined number of iterations $Iter_{GTS}$.

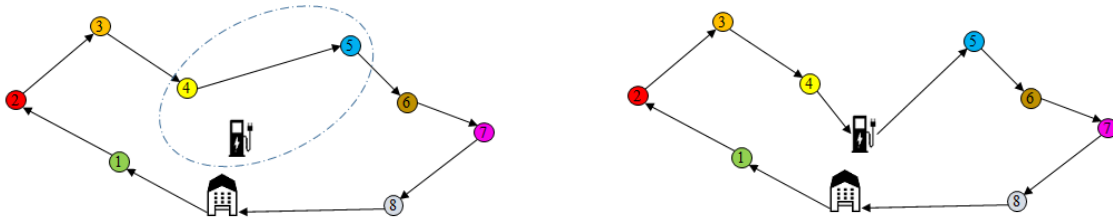
The neighborhood operators consist of the following six moves: 1-0 *Move*, 1-1 *Exchange*, 2-*Opt*, 2-*Opt*^{*}, 1-*AddRecharge*, and 1-*DropRecharge*. The first four moves are well-known operators in the literature and the last two are problem-specific operators inspired from Schneider et al. (2014). In 1-0 *Move* a customer node is removed from its position and inserted in another position while in 1-1 *Exchange* the positions of two customer nodes are swapped. Both moves are applied using both intra-route and inter-route schemes. 2-*Opt* prevents the formation of crisscross arcs in a route by breaking two arcs and reconnecting the break points with two new arcs while reversing the sequence of the nodes visited in between (Fig. 5.a).



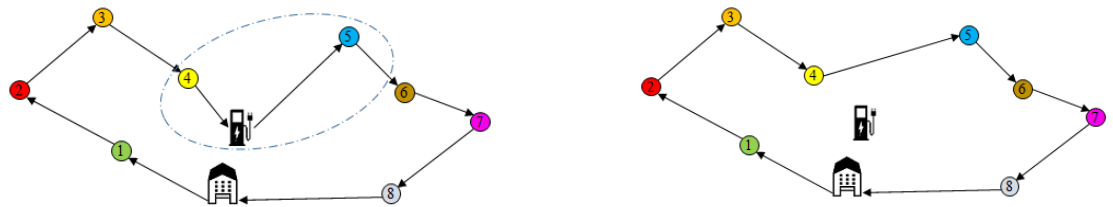
(a) *2-Opt* operator



(b) *2-Opt** operator



(c) *1-AddRecharge* operator



(d) *1-DropRecharge* operator

Fig. 5. Local search operators

2-Opt^* is an inter-route move adapted from 2-Opt (Potvin and Rousseau, 1995). It breaks two arcs belonging to two different routes and reconnects the first segment of the first route with the second segment of the second route and vice versa without reversing the sequence of the nodes (Fig. 5.b). Note that these operators are applied to the locations of the customers visited by the existing routes and the alternative locations are not considered. The 1-AddRecharge move inserts a recharging visit in the best position along the route. Since the chargers are only available in the depot, this move returns the vehicle to the depot for recharging (Fig. 5.c). The 1-DropRecharge move removes the visit for recharging from the route, if any exists (Fig. 5.d). If the vehicle recharges multiple times, it removes the one that decreases the current distance the most. All neighborhood operators are explored granularly and the best most is performed.

The tabu condition for each of the neighborhood operators is defined to prevent returning to previously explored solutions. In 1-0 Move , 2-Opt , and 1-1 Exchange moves if the position(s) of customer node (nodes) is (are) changed (swapped), it then cannot be changed (re-swapped) again by the same operator. In the 1-AddRecharge (1-DropRecharge) move, the inserted (removed) recharging cannot be removed (inserted) from (into) the route.

To reduce the computational effort, we employ GTS that evaluates promising moves only and omits a significant number of unpromising ones. This approach considers an arc or a node in a move if its cost does not exceed the granularity threshold defined as $\varphi = \frac{Z}{n+v}$, where Z represents the objective function value of the initial solution, n and v are the numbers of customers and routes in the solution, respectively. The granularity threshold is updated after every $Iter_G$ iterations by setting the threshold to $\varphi' = \frac{Z'}{(n'+v')}$, where Z' , v' and n' denote the objective function value, number of routes, and number of customers of the best solution obtained by GVNS/GTS, respectively. GTS is supported by an intensification strategy to improve the new incumbent solution (Hirsch and Gronalt, 2007; Aras et al., 2011). When we find a new incumbent solution, we apply 3-Opt as a local post-optimization procedure in an attempt to further improve it. 3-Opt breaks three arcs and replaces them with other three within a route.

5. Experimental study

In this section, we first describe the benchmark data sets that we used in our experiments and present the parameter tuning procedure based on a subset of VRPRDL instances from Ozbaygin

et al. (2017) and newly generated EVRP-FD instances. Next, we assess the performance of VNS/GTS using the VRPRDL instances by comparing its results with the branch-and-price algorithm of Ozbaygin et al. (2017). Then, we solve EVRP-FD instances with the VNS/GTS. For small-size instances, we use Gurobi for solving the mathematical model given in Section 3 and confirm the performance of the VNS/GTS by comparing its results with the ones obtained by the Gurobi solver. For medium and larger instances, we summarize our best solutions as benchmarks for future study. Finally, we perform a trade-off analysis concerning some parameters of the problem. All experiments were conducted on a computer outfitted with Intel Core i7-8700 3.2 GHz CPU and 32 GB DDR4 RAM. VNS/GTS was implemented in C# in Microsoft® Visual Studio 2019.

5.1. Data generation

We carry out our experiments using two sets of VRPRDL test problems employed by Ozbaygin et al. (2017). VRPRDL considers traditional vehicles with unlimited driving range. The first set includes 40 instances generated by Reyes et al. (2017) and modified by Ozbaygin et al. (2017). These instances involve 15 to 120 customers where customers have up to five roaming delivery locations. The second set includes 20 medium-size instances introduced in Ozbaygin et al. (2017) and involves 40 customers with up to five delivery locations. In all the instances, the X-Y coordinates of the customer locations were generated randomly in a square-shaped area lying within $[-200, 200]$.

To determine the EV-related parameters, we consider the electric Fiat Ducato (eDucato) in our computational study. Equipped with a 62 kWh battery the eDucato has a factory published driving range of 200 km (bedeo.co.uk). The driving range and battery performance can be affected by several factors such as temperature, cargo weight, road gradient, etc. (Rastani et al., 2020). So, we assume an actual driving range of 130 km. Since the EVs operate within 10%-90% of their battery capacity, the operational battery capacity is set to $62 \times 0.8 \approx 50$ kWh. Hence, the operational driving range is equal to $130 \times 0.8 \approx 100$ km, which translates into a discharge rate of 0.5 kWh/km. We assume fast chargers with 50 kW power.

Note that for a given driving range (100 km) some customers in the VRPRDL instances cannot be served, making those particular instances infeasible. To make them feasible, we had to modify the

coordinates of the customers' locations in the original VRPRDL instances in such a way that at least one of the delivery locations of each customer is located within the feasible driving range. In order to achieve the feasibility, we divided all the coordinates in the original data by four, which is the minimum integer value that makes all customers reachable. Ozbaygin et al. (2017) assumed a planning horizon of 12 hours and vehicle capacity of 750. However, the shortened distances created an imbalance between the tour duration and cargo capacity in our case, resulting in with many EVs returning to depot too early because of the tight capacity (or large cargo sizes). So, we kept the planning horizon same but set the EV capacity to 1500.

Table 2. Parameter tuning

Parameter	Values ($\Delta\%$)					
	5	10	15	20	25	30
η	5 (0.14)	10 (0.06)	15 (0.02)	20 (0.00)	25 (0.00)	30 (0.00)
α	0.1 (0.04)	0.2 (0.01)	0.5 (0.00)	1 (0.00)	1.5 (0.00)	-
β	0.1 (0.03)	0.2 (0.01)	0.5 (0.00)	1 (0.00)	1.5 (0.00)	-
γ	0.1 (0.04)	0.2 (0.02)	0.5 (0.00)	1 (0.00)	1.5 (0.00)	-
δ	0.1 (0.03)	0.25 (0.00)	0.5 (0.00)	0.75 (0.00)	-	-
$Iter_{GTS}$	20 (0.05)	50 (0.00)	100 (0.00)	150 (0.00)	-	-
$Iter_G$	n (0.09)	$2n$ (0.05)	$3n$ (0.00)	$4n$ (0.00)	$5n$ (0.00)	-
$Iter_{NonImp}$	100 (0.12)	300 (0.08)	500 (0.00)	1000 (0.00)	1500 (0.00)	-
$Iter_{Total}$	1000 (0.13)	2000 (0.06)	5000 (0.00)	10000 (0.00)	15000 (0.00)	-

5.2. Parameter tuning

VNS/GTS employs nine parameters including tabu duration (η), three penalty parameters for constraint violations (α, β, γ), an auxiliary parameter to update these penalties (δ), iteration counter for applying GTS ($Iter_{GTS}$), iteration counter for updating granularity threshold ($Iter_G$), number of non-improving iterations ($Iter_{NonImp}$), and the total number of iterations ($Iter_{Total}$). To tune these parameters, we selected instances 4, 10, 20, 30, and 35 from the VRPRDL data set and 6, 15, 25, 30, and 35 from the newly generated EVRP-FD data set. Our aim was to include instances with

different sizes. The number of customers in these instances varies between 15 and 120. The parameters were tuned in the sequence above from η to $Iter_{Total}$.

All parameters were initially set to the lowest values given in Table 2. We first considered six different η values, performed 10 runs for each instance, and calculated the average percentage deviation from the best solution ($\Delta\%$). Then, the parameter was fixed to the value that produced the smallest $\Delta\%$ (e.g. η is set to 20). We repeated this procedure for the remaining parameters until all of them had been tuned. If two parameter values produced the same $\Delta\%$, the smaller value was selected. Table 2 provides the obtained $\Delta\%$ for each of the corresponding parameter values. The selected parameter values are shown in bold. Note that in row $Iter_G$, n indicates the number of customers.

5.3. Computational results for the VRPRDL instances

In this section, we evaluate the performance of VNS/GTS on the VRPRDL instances of Ozbaygin et al. (2017). We modified our algorithm to solve the VRPRDL by removing the driving range feasibility check and recharge-related operators. Basically, we employed λ -*SwitchLocation* and *Merge* operators in shaking and 1-0 *Move*, 1-1 *Exchange*, 2-*Opt*, and 2-*Opt*^{*} operators in GTS. We also set $F = 0$ to only minimize the total distance travelled, as is the case in the VRPRDL.

Table 3. Average results for the VRPRDL instances

n	Avg #Loc	Avg Optimal	VNS/GTS				
			Best	Avg	Best $\Delta\%$	Avg $\Delta\%$	Avg t(s)
≤ 30	3.57	1575.75	1575.75	1576.50	0.00	0.04	27.92
40	3.93	2585.05	2587.35	2589.10	0.09	0.16	133.36
60	3.74	3721.30	3724.80	3728.70	0.10	0.21	280.95
120	3.73	5373.80	5403.00	5406.00	0.56	0.61	1163.54
Average		3313.98	3322.73	3325.08	0.19	0.26	401.44

Table 3 presents the average results for the 60 VRPRDL instances, in comparison with the optimal solutions obtained by the branch-price-and-cut algorithm of Tilk et al. (2021). In this table, the first two columns denoted by “ n ” and “Avg #Loc” indicate the number of customers and the average number of customer delivery locations, respectively. The third column “Avg Optimal” reports the optimal solutions obtained by the branch-price-and-cut algorithm of Tilk et al. (2021). The remaining five columns under “VNS/GTS” present our solutions, where “Best” and “Avg.”

refer to the averages of the best and average objective function values (OFVs) over 10 runs, respectively. “Best $\Delta\%$ ” and “Avg. $\Delta\%$ ” represent the average percentage deviations of the best and average OFVs from the optimal solution with respect to number of customers, respectively. Finally, the last column provides the average CPU time in seconds.

VNS/GTS can find the optimal solution in 34 out of 60 instances in this data set. Note that VNS/GTS was able to find the optimal solutions in all the small-size instances involving 15 to 30 customers. For the instances with $n \leq 30$, the average deviations of the best and average solutions from optimal solutions are 0.00% and 0.04%, respectively. The average deviations of the best solutions from optimal solutions for the instances with $n = 40, 60,$ and 120 are 0.09%, 0.10%, and 0.56%, respectively while the average deviations of the average solutions are 0.16%, 0.21% and 0.61%, respectively. These deviations reflect the good performance and robustness of our proposed method. Regarding the computational effort, we notes that our average CPU times for the instances with $n \leq 30$ is 27.92 seconds, whereas for the instances with $n = 40, 60,$ and 120 the CPU times are 133.36, 280.95, and 1163.54 seconds, on average, respectively. Overall, our results show that VNS/GTS is capable of finding high-quality solutions within reasonable computation times. The detailed results for the whole dataset of VRPRDL instances are provided in Appendix A.

5.4. Computational results for EVRP-FD instances

To further assess the performance of VNS/GTS, we solved the small-size EVRP-FD instances using Gurobi 9.1 with a two-hour time limit and compared the results in Table 4. In this table, “#Veh” represents the number of vehicles and columns “UB”, “Gap%”, and “t(s)” under “Gurobi” report the upper bound, percentage optimality gap (“Gap%”), and run time in seconds, respectively. If Gurobi terminates within the 2-hour time limit, then the upper bound is optimal. The columns “Best”, “t(s)”, and “Best $\Delta\%$ ” under VNS/GTS show the best OFV over 10 runs, the percentage gap between our best OFV and upper bound given by Gurobi, and average CPU time in seconds, respectively. As in Table 4, the optimal solutions are indicated in bold and the VNS/GTS solutions that are better than the upper bounds are highlighted in bold and underlined.

Table 4. Results for small-size EVRP-FD instances

Instance	n	Avg #Loc	#Veh	Gurobi			VNS/GTS			
				UB	Gap%	t(s)	#Veh	Best	t(s)	Best $\Delta\%$
1	15	4.07	1	194.13	0.00	89	1	194.13	6.68	0.00
2	15	3.73	1	237.18	0.00	2572	1	237.18	4.98	0.00
3	15	3.40	1	224.68	0.00	5047	1	224.68	5.95	0.00
4	15	3.27	1	209.38	0.00	284	1	209.38	2.62	0.00
5	15	3.40	2	338.63	47.50	7200	2	338.63	8.04	0.00
6	20	3.25	2	279.20	48.58	7200	2	<u>250.55</u>	6.27	<u>-10.26</u>
7	20	3.35	2	238.63	48.73	7200	2	238.63	5.72	0.00
8	20	3.95	2	250.25	48.04	7200	2	250.25	6.62	0.00
9	20	3.75	2	255.63	47.82	7200	2	<u>248.00</u>	12.62	<u>-2.98</u>
10	20	3.10	2	277.33	48.31	7200	2	<u>261.78</u>	8.77	<u>-5.61</u>
11	30	3.40	3	429.33	65.34	7200	3	<u>401.43</u>	24.21	<u>-6.50</u>
12	30	3.73	3	421.40	65.18	7200	3	<u>362.25</u>	30.33	<u>-14.04</u>
13	30	3.90	3	315.83	32.67	7200	<u>2</u>	355.33	23.71	-
14	30	3.53	3	377.42	65.55	7200	3	<u>274.48</u>	26.37	<u>-27.28</u>
15	30	4.10	3	327.03	32.95	7200	3	<u>320.83</u>	27.53	<u>-1.90</u>
16	30	3.93	2	343.13	48.80	7200	2	343.13	25.18	0.00
17	30	4.30	3	419.97	65.04	7200	3	<u>382.60</u>	36.53	<u>-8.90</u>
18	30	3.50	3	428.33	33.23	7200	3	<u>405.58</u>	20.99	<u>-5.31</u>
19	30	3.23	3	320.33	65.01	7200	3	<u>319.78</u>	16.24	<u>-0.17</u>
20	30	2.47	2	439.23	48.98	7200	2	<u>389.15</u>	13.34	<u>-11.40</u>
Average					40.59	6160			15.64	<u>-4.97</u>

In Table 4, we observe that Gurobi solved only four instances out of 20 to optimality within two hours and its average run time on these four instances is 1998 seconds. Given the fact that Gurobi is a general-purpose solver, this is an expected result considering the complexity of the problem. VNS/GTS matched the optimal solution in those four instances and produced better solutions in remaining 16 with an average gap of -4.97% . Note that in instance “13”, VNS/GTS was able to find a solution with a smaller fleet size compared to the solution of Gurobi. Note also that the average CPU time of the VNS/GTS is only 16 seconds. The results of 20 medium-size and 20 large-size EVRP-FD instances are presented in Table 5. The average CPU time is 54 seconds and the average gap between the average and best solutions is 0.15% for medium-size instances whereas for large-size instances they are 402 seconds and 0.19% , respectively. In total, for medium- and large-size EVRP-FD instances, the average CPU time is 228 seconds and the average gap is 0.17% . The small gap values reflect the robustness of the proposed VNS/GTS.

Table 5. Results for medium- and large-size EVRP-FD instances

Instance	n	Avg loc.	#Veh	Best	Avg	t(s)	$\Delta\%$	Instance	n	Avg loc.	#Veh	Best	Avg	t(s)	$\Delta\%$
41_v1	40	3.98	3	605.40	605.67	50.23	0.04	21	60	3.73	6	634.10	635.36	133.99	0.20
42_v1	40	3.93	3	531.10	531.76	52.55	0.12	22	60	3.53	4	466.48	466.58	90.84	0.02
43_v1	40	4.05	2	453.53	454.15	48.12	0.14	23	60	3.90	6	607.45	609.51	170.79	0.34
44_v1	40	3.53	2	446.22	446.97	28.79	0.17	24	60	3.80	4	618.30	619.60	105.37	0.21
45_v1	40	3.60	4	554.93	556.05	46.35	0.20	25	60	3.88	5	530.90	530.94	91.63	0.01
46_v1	40	4.33	4	606.65	606.80	69.55	0.02	26	60	3.73	6	599.30	599.63	94.93	0.05
47_v1	40	4.18	4	555.93	556.76	58.45	0.15	27	60	3.45	5	571.62	573.21	102.36	0.28
48_v1	40	3.83	4	682.70	683.02	77.61	0.05	28	60	3.63	5	527.35	528.91	113.28	0.30
49_v1	40	3.80	3	709.60	711.52	86.93	0.27	29	60	3.75	5	558.33	559.68	173.72	0.24
50_v1	40	4.03	3	487.83	488.86	38.13	0.21	30	60	3.95	6	615.13	616.29	97.00	0.19
41_v2	40	3.98	4	483.50	484.96	73.61	0.30	31	120	3.83	8	740.30	742.99	485.06	0.36
42_v2	40	3.93	3	397.30	397.52	45.37	0.06	32	120	3.67	8	807.80	807.90	735.58	0.01
43_v2	40	4.05	3	411.60	411.63	55.12	0.01	33	120	3.92	7	766.65	770.53	835.75	0.51
44_v2	40	3.53	3	336.85	337.75	31.42	0.27	34	120	3.78	8	877.60	879.97	610.70	0.27
45_v2	40	3.60	3	430.33	431.70	53.94	0.32	35	120	3.75	7	722.90	725.12	518.50	0.31
46_v2	40	4.33	4	430.93	432.08	52.95	0.27	36	120	3.51	8	932.33	935.28	698.21	0.32
47_v2	40	4.18	3	421.90	422.50	44.40	0.14	37	120	3.88	8	754.97	755.77	689.45	0.11
48_v2	40	3.83	3	557.63	558.16	54.11	0.10	38	120	3.51	7	921.73	921.96	647.84	0.03
49_v2	40	3.80	4	527.67	527.87	52.39	0.04	39	120	3.56	9	865.93	866.75	815.05	0.10
50_v2	40	4.03	4	416.41	507.70	55.10	0.13	40	120	3.84	8	744.55	744.96	828.17	0.06
Average						53.76	0.15	Average						401.91	0.19

5.5. Effect of hybridizing VNS and GTS

In the local search phase of VNS/GTS, we allow non-improving moves using the TS mechanism in an attempt to enhance the performance of the VNS algorithm. To investigate the contribution of this hybrid approach on the algorithmic performance, we also implemented the pure VNS and GTS versions by prohibiting the non-improving moves during the local search and by removing the shaking mechanisms, respectively. We selected a subset of ten large-size EVRP-FD instances (instances 21, 23, 25, 27 and 29 with 60 customers and instances 31, 33, 35, 37 and 39 with 120 customers), repeated our experiments using these two methods, and compared the results. In order to ensure a fair comparison with respect to the computational effort, we removed the limit on the number of iterations in VNS and GTS, and stopped them when the run times of VNS/GTS reported in Table 5 had been reached.

Table 6. Comparison of results obtained by using VNS/GTS, GTS and VNS

Instance	VNS/GTS		GTS		VNS	
	#Veh	Best	#Veh	Best	#Veh	Best
21	6	634.10	<u>5</u>	672.32	6	654.56
23	<u>6</u>	607.45	<u>6</u>	660.88	7	641.47
25	<u>5</u>	530.90	<u>5</u>	533.31	6	585.20
27	<u>5</u>	571.62	6	572.92	6	571.03
29	<u>5</u>	558.32	6	586.93	<u>5</u>	584.34
31	<u>8</u>	740.30	9	796.22	<u>8</u>	738.23
33	<u>7</u>	766.65	9	757.06	8	707.53
35	<u>7</u>	722.90	8	769.89	9	746.81
37	<u>8</u>	754.97	9	836.57	9	813.03
39	<u>9</u>	865.92	10	897.56	10	875.99
Average	6.6		7.3		7.4	

The results are provided in Table 6. Since the primary objective is to minimize the number of vehicles, we report smaller fleet sizes in bold and underlined, whereas the best OFVs corresponding to the solutions with smallest fleet sizes are shown in bold. The results show that VNS/GTS outperforms both VNS and GTS in eight instances by producing solutions that require minimum number of vehicles. Furthermore, in all these eight instances, the total travel distances are shorter than those of VNS and/or GTS. In only one instance, GTS achieved a fleet with one vehicle less. This may be due to the better exploitation of the solution space through a longer local search

procedure. Furthermore, in another instance VNS found a solution with shorter total distance but the difference is only 0.28%. Overall, we can conclude that VNS/GTS algorithm benefits from the implementation of TS mechanism within the VNS procedure in producing high-quality solutions.

5.6. Trade-off analysis

This section provides the trade-off analysis concerning key parameters of the EVRP-FD including the fixed cost incorporated in the objective function to reduce the fleet size, vehicle cargo capacity, recharging rate, and the battery capacity. Furthermore, we provide a comparison of the multiple delivery locations against a single delivery location case to observe the benefits of flexible deliveries. We also investigate the availability of multiple (public) recharging stations on the delivery plans. These analyses are based on the same large-size instances used in Section 5.5. Our analyses throughout this subsection mainly focus on the trade-offs associated with fleet size (#Veh), total number of recharges performed en-route (#Rech), and total distance travelled (TD). All results are based on the best solutions obtained after performing 10 runs.

5.6.1. Influence of fixed cost

We associated each vehicle with a sufficiently large constant (fixed cost) F in the objective function (1) to reduce the fleet size. Removing the fixed cost from the objective function minimizes the total distance travelled independently from the number of vehicles. So, we set $F = 0$ and solved a subset of instances again to compare the route plans generated for the two objectives. Our preliminary results showed that the algorithm may suffer from the removal of the fixed cost. We observed this particularly when the two objectives do not conflict, i.e. shorter distances are achieved with smaller-size fleets. The reason is because the penalties associated with the violations of the constraints may be compensated by a decrease in the fleet size, allowing the algorithm to better exploit the infeasible regions of the search space when $F > 0$. Therefore, we decided to initiate the algorithm with $F > 0$ in an attempt to find a good solution with minimum number of vehicles, and then set $F = 0$ to minimize the total distance. This strategy enhanced the performance of the algorithm because it is equipped with neighborhood structures that can increase the fleet size in order to reduce the total distance in the case of conflicting objectives.

Table 7. Comparison of results obtained with and without fixed cost

Instance	n	$F > 0$			$F = 0$		
		#Veh	#Rech	TD	Δ #Veh	Δ #Rech	Δ TD (%)
21	60	6	2	634.10	1 ↗	2 ↘	8.45 ↘
23	60	6	2	607.45	1 ↗	2 ↘	1.09 ↘
25	60	5	2	530.90	1 ↗	2 ↘	5.87 ↘
27	60	5	2	571.62	1 ↗	2 ↘	4.76 ↘
29	60	5	2	558.32	1 ↗	2 ↘	2.44 ↘
31	120	8	1	740.30	–	–	–
33	120	7	4	766.65	1 ↗	4 ↘	5.36 ↘
35	120	7	3	722.90	–	–	–
37	120	8	1	754.97	1 ↗	1 ↘	3.17 ↘
39	120	9	2	865.92	1 ↗	2 ↘	0.44 ↘
Average		6.6	2.1	675.32	0.8 ↗	1.7 ↘	2.98 ↘

The results are summarized in Table 7. Although the solution of problems “31” and “35” did not change the removal of the fixed cost lead to increased fleet size in most of the instances, which in turn resulted in a major reduction in the recharges. We observe that in most of the instances, the vehicles do not recharge en-route. This is an expected outcome because, in a larger fleet, vehicles serve fewer customers on average and travel shorter distances. In addition, dispatching more vehicles brings no additional cost when $F = 0$, whereas detours for recharging may increase the tour lengths significantly. Overall, the total distance are reduced by almost 3%, on average, when the costs of the vehicles are omitted. On the other hand, the fleet size increases by 13%, on average, and the average number of recharges reduces by 81%. So, the savings in distance can be associated with the need for less frequent recharges.

Table 8. Comparison of results with respect to different cargo capacities

Instance	$C = 1000$			$C = 2000$		
	Δ #Veh	Δ #Rech	Δ TD (%)	Δ #Veh	Δ #Rech	Δ TD (%)
21	–	–	2.23 ↗	–	–	–
23	–	–	10.95 ↗	–	–	–
25	–	1 ↗	23.91 ↗	–	–	–
27	1 ↗	1 ↘	0.62 ↘	–	–	–
29	–	1 ↘	1.06 ↘	–	–	0.90 ↘
31	1 ↗	1 ↘	7.25 ↗	–	–	0.68 ↘
33	1 ↗	4 ↘	10.35 ↘	–	–	0.98 ↘
35	–	1 ↘	4.80 ↗	–	–	–
37	–	1 ↗	11.94 ↗	–	–	–
39	–	1 ↘	4.69 ↗	–	–	–
Average	0.3 ↗	0.7 ↘	5.00 ↗	–	–	0.26 ↘

5.6.2. Influence of vehicle cargo capacity

The vehicle cargo capacity was set to $C = 1500$ in the experimental study. We repeated our experiments by considering $C = 1000$ and $C = 2000$ to investigate the impact of using smaller and larger vehicles on the routing decisions. The results are presented in Table 8. We observe that increasing the capacity has almost no influence on the solutions: the fleet compositions and the recharging decisions remained same and the total distance improved only by 0.26% on average. These results show that the length of the planning horizon poses a more restrictive limitation in the problem. On the other hand, reducing the capacity increases either the fleet size or total distance in all the instances except for “29”. In addition, the average increases in the number of vehicles and total distance are 4.55% and 5.00%, respectively. We also see that the average number of recharges decreases by 33% due to the utilization of a larger fleet.

5.6.3. Influence of charger type

In our experiments, we considered fast chargers with power rate of 50 kW. To investigate the effects of different charger types on the delivery plans, we repeated our experiments by utilizing a slower charger with 22 kW power as well as a super-fast charger with 150 kW power, which correspond to 130 and 20 minutes of recharge duration, respectively, from an empty battery to full capacity for the eDucato considered in this study.

Table 9. Comparison of results with respect to different charger types

Instance	22 kW			150 kW		
	Δ #Veh	Δ #Rech	Δ TD (%)	Δ #Veh	Δ #Rech	Δ TD (%)
21	–	1 \Downarrow	4.84 \Uparrow	1 \Downarrow	1 \Uparrow	9.43 \Downarrow
23	1 \Uparrow	1 \Downarrow	32.68 \Uparrow	1 \Downarrow	1 \Uparrow	8.95 \Uparrow
25	1 \Uparrow	1 \Downarrow	29.16 \Uparrow	–	–	1.09 \Downarrow
27	1 \Uparrow	1 \Downarrow	3.33 \Uparrow	1 \Downarrow	–	3.77 \Downarrow
29	–	1 \Downarrow	20.06 \Uparrow	–	–	0.55 \Downarrow
31	1 \Uparrow	1 \Downarrow	0.80 \Uparrow	1 \Downarrow	1 \Uparrow	4.48 \Uparrow
33	1 \Uparrow	2 \Downarrow	3.30 \Downarrow	–	1 \Uparrow	0.74 \Downarrow
35	1 \Uparrow	1 \Downarrow	4.05 \Uparrow	–	–	1.51 \Downarrow
37	–	–	1.93 \Uparrow	1 \Downarrow	1 \Uparrow	3.26 \Uparrow
39	1 \Uparrow	2 \Downarrow	2.25 \Uparrow	1 \Downarrow	1 \Uparrow	3.10 \Uparrow
Average	0.7 \Uparrow	1.1 \Downarrow	8.28 \Uparrow	0.6 \Downarrow	0.6 \Uparrow	0.48 \Uparrow

Table 9 depicts the results. As expected, when the recharges are faster a smaller fleet is operated with more frequent recharges en-route whereas the opposite is observed with slower chargers. In the case of super-fast chargers, the fleet size decreases by 9.09% on average while the number of recharges and total distance increase by 28.57% and 0.48%, respectively. Note that decreasing the fleet size can result in increasing the total distance in some instances. On the other hand, when slower chargers are available, the fleet size and total distance go up, on average, by 10.61% and 8.28%, respectively, whereas the number of recharges go down by 52.38%.

5.6.4. Influence of vehicle battery capacity

Our experiments were based on eDucato EVs equipped with a 62 kWh battery. To investigate the impact of the battery size on the solutions, we performed further experiments by considering EVs with 80 and 100 kWh batteries. The comparative results are provided in Table 10. Increasing the battery capacity leads to the utilization of a smaller fleet. This is an expected result since larger battery means extended driving range, which, in turn, allows the EVs visit more customers along their routes. Consequently, the total distances also decrease significantly in many instances. An 80 kWh battery reduces the fleet size and total distance, on average, by 12.12% and 6.93%, respectively, whereas the decreases are 24.24% and 9.16%, respectively, when the EVs have a 100 kWh battery. We observe that the number of recharges en-route decrease as well, by 85.71% and 95.24% in the case of 80 and 100 kWh EVs, respectively. It is also worth noting that when the EVs are equipped with a 100 kWh battery, none of the vehicles needed recharging in nine instances.

Table 10. Comparison of results with respect to different battery sizes

Instance	80 kWh			100 kWh		
	Δ #Veh	Δ #Rech	Δ TD (%)	Δ #Veh	Δ #Rech	Δ TD (%)
21	1 \downarrow	2 \downarrow	16.58 \downarrow	2 \downarrow	2 \downarrow	21.94 \downarrow
23	1 \downarrow	2 \downarrow	11.56 \downarrow	2 \downarrow	2 \downarrow	14.57 \downarrow
25	1 \downarrow	1 \downarrow	4.32 \uparrow	1 \downarrow	2 \downarrow	12.38 \downarrow
27	–	2 \downarrow	18.12 \downarrow	1 \downarrow	2 \downarrow	19.25 \downarrow
29	–	2 \downarrow	1.67 \downarrow	–	2 \downarrow	5.58 \downarrow
31	1 \downarrow	1 \downarrow	4.43 \downarrow	3 \downarrow	–	1.53 \uparrow
33	1 \downarrow	3 \downarrow	7.53 \downarrow	1 \downarrow	4 \downarrow	10.77 \downarrow
35	–	3 \downarrow	3.82 \downarrow	1 \downarrow	3 \downarrow	1.01 \downarrow
37	1 \downarrow	1 \downarrow	1.99 \downarrow	2 \downarrow	1 \downarrow	1.90 \uparrow
39	2 \downarrow	1 \downarrow	8.00 \downarrow	3 \downarrow	2 \downarrow	13.79 \downarrow
Average	0.8 \downarrow	1.8 \downarrow	6.93 \downarrow	1.6 \downarrow	2 \downarrow	9.16 \downarrow

5.6.5. Multiple delivery locations vs. single delivery location

In the EVRP-FD the customers have the flexibility to have their orders delivered at pre-determined alternative locations and times throughout the day. To investigate the benefits of flexible deliveries to route planning we solved the selected instances in the single delivery case again by considering two scenarios. In the first scenario, we randomly selected one location along with the associated time window among the alternative locations. In the second scenario, we selected the home location (first location) of each customer by assuming a time window $[0, l_0]$, where l_0 is the closing time of the depot (i.e. the delivery can be performed any time during the day).

Table 11. Comparison of results with respect to delivery options

Instance	Randomly Selected Location			Home Location		
	Δ #Veh	Δ #Rech	Δ TD (%)	Δ #Veh	Δ #Rech	Δ TD (%)
21	1 ↗	–	20.36 ↗	3 ↘	2 ↗	1.10 ↗
23	3 ↗	1 ↘	44.45 ↗	3 ↘	3 ↗	19.54 ↗
25	2 ↗	–	36.61 ↗	2 ↘	2 ↗	11.79 ↗
27	3 ↗	2 ↘	23.92 ↗	2 ↘	1 ↗	7.81 ↗
29	3 ↗	–	58.22 ↗	2 ↘	4 ↗	37.7 ↗
31	4 ↗	1 ↗	72.17 ↗	4 ↘	4 ↗	26.07 ↗
33	4 ↗	1 ↘	43.77 ↗	2 ↘	–	6.82 ↗
35	4 ↗	1 ↘	44.95 ↗	3 ↘	1 ↗	7.48 ↗
37	5 ↗	1 ↗	74.36 ↗	4 ↘	4 ↗	26.38 ↗
39	4 ↗	–	60.59 ↗	5 ↘	5 ↗	19.46 ↗
Average	3.3 ↗	0.3 ↘	49.40 ↗	3 ↘	2.6 ↗	16.44 ↗

The results summarized in Table 11 show that the single delivery location option increases the total distance in both scenarios as expected; however, the increase is dramatic in the first scenario with 49.40%, on average, whereas it is 16.44%, on average, in the second scenario. This significant difference is due to the wide time windows allowed for home deliveries, which provides considerable flexibility to the delivery company at the expense of increased customer dissatisfaction. Note that the time window flexibility in the second scenario also allows major reduction in the fleet size. While the number of EVs decreases by 45% on average in the second scenario, a 50% larger fleet, on average, is needed in the first scenario. In sum, we can conclude that flexible deliveries can improve overall customer satisfaction from the service offered and bring significant cost savings to the logistics operator.

5.6.6. Multiple recharging stations vs. recharging only at depot

We assumed that the EVs are recharged only at the depot because of various operational limitations. In this section, we relax this assumption and investigate the effect of allowing recharges in public stations. To do this, we considered two cases involving five and 10 recharging stations, all with 50 kW power. We determined the station locations randomly by dividing the delivery area into four equal-size zones to make sure that they are geographically dispersed. The station locations remained same in the instances with same size.

Table 12. Comparison of results with respect to different recharging policies

Instance	5 stations			10 stations		
	Δ #Veh	Δ #Rech	Δ TD (%)	Δ #Veh	Δ #Rech	Δ TD (%)
21	1 \downarrow	1 \uparrow	13.67 \downarrow	1 \downarrow	3 \uparrow	14.17 \downarrow
23	–	–	1.59 \downarrow	2 \downarrow	1 \uparrow	11.28 \downarrow
25	–	1 \uparrow	1.81 \downarrow	1 \downarrow	2 \uparrow	3.51 \downarrow
27	–	2 \uparrow	5.38 \downarrow	1 \downarrow	2 \uparrow	6.49 \downarrow
29	–	2 \uparrow	1.51 \downarrow	1 \downarrow	3 \uparrow	5.02 \downarrow
31	1 \downarrow	2 \uparrow	2.61 \downarrow	2 \downarrow	2 \uparrow	3.31 \downarrow
33	–	–	4.10 \downarrow	1 \downarrow	1 \uparrow	7.50 \downarrow
35	–	–	1.61 \downarrow	1 \downarrow	1 \uparrow	2.63 \downarrow
37	1 \downarrow	2 \uparrow	2.10 \downarrow	2 \downarrow	2 \uparrow	7.26 \downarrow
39	1 \downarrow	–	3.02 \downarrow	1 \downarrow	1 \uparrow	4.05 \downarrow
Average	0.4 \downarrow	1 \uparrow	3.70 \downarrow	1.3 \downarrow	1.8 \uparrow	6.41 \downarrow

Table 12 summarizes the results. As expected, the availability of public recharging stations improves the solutions both in terms of the distance travelled and fleet size. Although the fleet sizes do not change in six instances and the average reduction is only 6.06% in the case of five stations, we observe substantial savings in fleet size in all 10-station instances with an average downsizing of 19.70%. On the other hand, the average decreases in total distance are 3.70% and 6.41% for the cases of 5- and 10-stations, respectively. These results reveal that the logistics companies can benefit from the availability of recharging at public stations **located in their delivery area**. To this end, **they can determine the most frequently used station locations** and negotiate a contract-based plan with the station operators for long-term relationship. Note that we also considered 20 stations but the results did not show much improvement compared to the 10-station case (on average, 0.1% in fleet size and 0.4% in total distance). So, we did not report them.

6. Case study

In this section, we present a case study based on Argos, a U.K. multi-channel retailer that offers more than 50,000 products with over 123 million transactions per year using catalogues and digital platforms. We consider Argos Bulwell depot located in the East Midlands area and determine 40 customers at randomly selected locations in Nottinghamshire, Derbyshire, Lincolnshire, and Loughborough counties. The sizes of the customer orders are uniformly distributed between 1 and 5 cubic feet. In the current practice, Argos delivers to a single location offering three alternative time slots of 7 AM–1 PM, 2 PM–6 PM, and 7 PM–11 PM. So, we randomly selected one of these slots to set the customer time windows. The data including the customer order sizes, location coordinates, and the delivery time windows are given in Table B.1 provided in the Appendix B. We assumed a delivery fleet consisting of eDucato EVs with a 62 kWh battery capacity and 530 cubic feet (15 m³) cargo cabin. The distances were calculated using the VRP Solver of Erdoğan (2017) based on the Bing Maps road network.

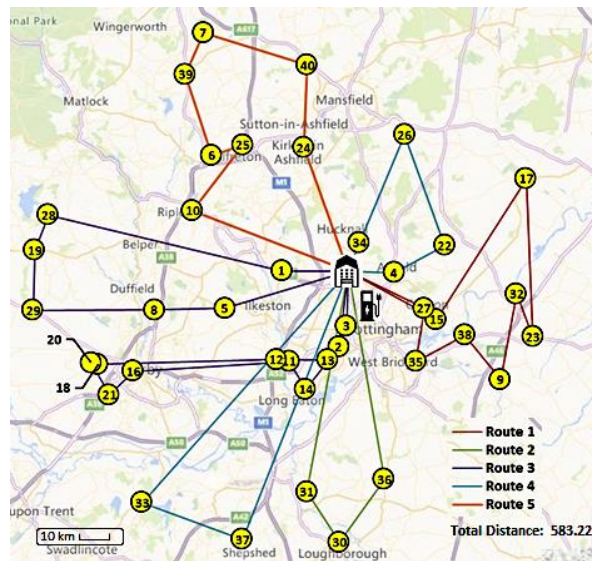


Fig. 6. Visualization of the routes in the current single delivery location setting

First, we determined the delivery plans for the current setting by solving the routing problem using VNS/GTS. The routes are illustrated in Fig. 6 and the detailed route plans are provided in Table C.1 provided in Appendix C. We see that five vehicles are employed to serve the customers while two need recharging to continue their routes. The total distance traveled is 583.22 km.



Fig. 7. The geographical locations of the depot and each customer alternative locations

To investigate the effect of flexible delivery service, we assigned alternative delivery locations to the majority of the customers by keeping their existing locations in the list. So, we randomly determined 55 additional delivery locations in the area where 15 customers were associated with two locations, 20 customers with three locations while the remaining five customers maintained their existing location preferences. To improve the customer satisfaction, we decided to set the delivery times between 9 AM and 9 PM since 7 AM–9 AM and 9 PM–11 PM deliveries tend to be uncomfortable for most people. So, we employed 3-hour delivery time slots: 9 AM–12 PM, 12 PM–3 PM, 3 PM–6 PM, and 6 PM–9 PM. For consistency, we ensured that the existing delivery time preferences overlap with one of these time windows. All locations are illustrated in Fig. 7 and the detailed data are provided in Table B.2 in Appendix B.

The solution for the flexible delivery case is depicted in Fig. 8 and the route plans are given in Table C.1 in Appendix C. The yellow nodes on the figure show the delivery locations whereas the green ones are the unvisited alternative locations. The results show that flexible deliveries save one EV in the fleet size compared to current practice. Furthermore, the total distance traveled decreases by 23%, which indicates a substantial reduction in fuel costs.

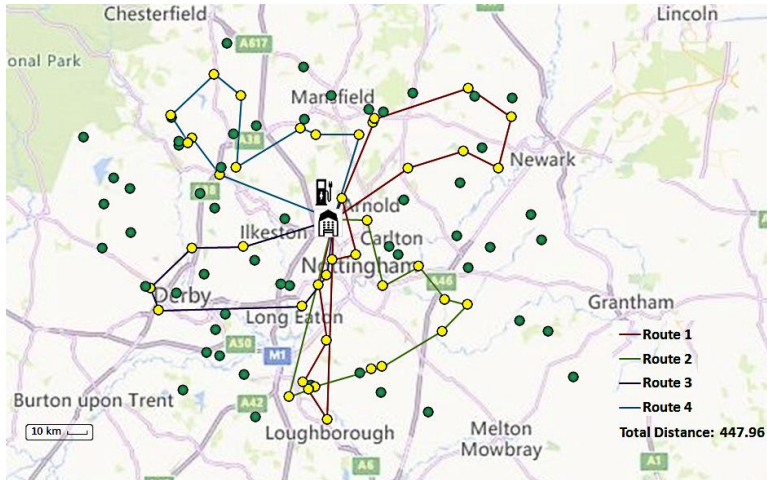


Fig. 8. Visualization of the solution obtained by VNS/GTS

We also considered 1- and 2-hour time window cases in an attempt to improve the customer satisfaction through reduced delivery time variability. We observed that the fleet size remains same with five EVs while the total distance decreases by 17% in the case of 2-hour delivery time slots. With 1-hour delivery time slots, one additional EV is needed in the fleet whereas the total distance reduces by 3%. From these results, we can conclude that 1-hour time slot option may not pay off the effort and can be operationally demanding. On the other hand, 1-hour time slot option may offer a good compromise to enhance the service quality and deserve further investigation.

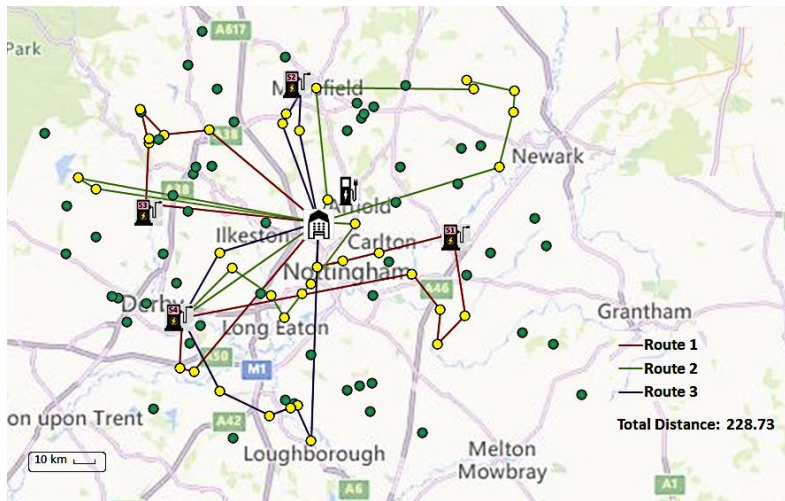


Fig. 9. Visualization of the routes for recharging in public stations

Finally, we investigated the impact of recharging at public stations on the route plans by considering 3-hour time windows with flexible deliveries. To this end, among the charging stations available in this area we randomly selected four stations equipped with 50 kW chargers. Their coordinates are provided in Table B.3 in Appendix B. The results are reported in Table C.1 in Appendix C and the routes are illustrated in Fig. 9. As opposed to the results reported in Section 5.5.6, we observe that the availability of public station charging has a tremendous effect on the total distance traveled, hence the fuel cost, pointing out a reduction of 49%. In addition, the fleet size reduces from four EVs to three. These results re-emphasize the importance of collaboration between the logistics operators and energy providers for their mutual benefits.

7. Concluding remarks and future research directions

In this study, we introduced the Electric Vehicle Routing Problem with Flexible Deliveries (EVRP-FD) as a variant of the well-known Electric Vehicle Routing Problem with Time Windows. In this problem, a homogenous fleet of commercial EVs dispatched from a single depot serves a set of customers with alternative delivery locations and time windows. The vehicles are allowed to recharge their batteries en-route. We formulated the mathematical programming model of the problem and developed a hybrid Variable Neighborhood Search method coupled with Tabu Search to solve it. We verified the performance of our method using benchmark instances of a similar problem from the literature. We also generated new EVRP-FD instances and performed numerical experiments to see the impact of problem parameters such as fixed vehicle acquisition cost, cargo capacity, recharging rate, and battery size on the route plans. In addition, we investigated the benefits of flexible deliveries and availability of public recharging stations to operational efficiency. We can summarize our findings as follows: (i) omitting vehicle acquisition cost has minor effect on the travel distances but leads to increased fleet size, which in turn allows fewer recharges en-route; (ii) the solutions are insensitive to the vehicle cargo capacity, i.e., the planning horizon is a more restrictive constraint; (iii) as expected, a smaller fleet is needed if the battery size is larger and/or fast chargers are available; (iv) offering flexible delivery service reduces both the fleet size and total distance travelled; and (vi) despite the operational limitations, the utilization of public recharging stations can be cost effective.

We presented a case study based on a major U.K. retailer using a data set from the East Midlands area as well. The results of this study supported our findings from the experimental study. We observed that flexible deliveries reduced the fleet size by 20% and fuel cost by 23%. We also revisited the availability of recharging at public stations located in the area. The results exhibited 25% reduction in fleet size and 49% reduction in fuel cost, and revealed that the operational costs can be cut down substantially if the logistics operators collaborate with energy companies.

Future research on this topic may address other EVRP variants by considering other flexible delivery options. For instance, a practical problem can incentivize alternative locations nominated by the company through various rewarding schemes to the consumers, e.g. allowing collections from dedicated collection points at reduced delivery rates. In addition, the customer satisfaction may be considered as a criterion and the trade-offs associated with delivery service quality and delivery location/time window options may be investigated. Most, if not all, of the studies on EVRP assume that the vehicle departs from the depot loaded with the entire cargo of all the customers assigned to its route. However, when an EVs returns to the depot for recharging, the demands of the remaining customers on its route can be loaded while the vehicle is charging, if time permits. This may be particularly important when the cargo weight is taken into account in the energy consumption and it may show significant differences in route plans and the related costs in the case delivering heavy goods.

If the problem involves a large fleet, the recharges at the depot may overlap. Then, the problem may be extended to incorporate the scheduling/queueing of the vehicles if the chargers are limited in quantity and/or power rate. Within this context, recharging at public recharging stations may be considered as well.

List of Figures

Fig. 1. An illustrative example

Fig. 1. Alt Text: In this figure, we present an illustrative example that involves 10 customers (shown in different colors) and 26 delivery locations. The nodes with the same ID number represent the alternative delivery locations of a customer (e.g. customer C1 has three alternative locations shown as nodes numbered “1” and highlighted in green). Two EVs depart from the depot for service. EV#1 returns to the depot for recharging in the midst of its tour while EV#2 completes its tour and returns to the depot without recharging.

Fig. 2. λ -SwitchLocation shaking operators

Fig. 2. Alt Text: Figure 2 illustrates the working mechanism of the *SwitchLocation* neighborhood operators. The illustrations on the left and on the right show the routes before and after the operator has been applied, respectively. Fig. 2(a) illustrates the 1-*SwitchLocation* move, Fig. 2(b) shows the 2-*SwitchLocation* move, and Fig. 2 (c) depicts the 3-*SwitchLocation* move.

Fig. 3. κ -MoveCustomer shaking operators

Fig. 3. Alt Text: Figure 3 illustrates the working mechanism of the *MoveCustomer* neighborhood operators. The illustrations on the left and on the right show the routes before and after the operator has been applied, respectively. Fig. 3(a) illustrates the 1-*MoveCustomer* move, Fig. 3(b) shows the 2-*MoveCustomer* move, and Fig. 3(c) depicts the 3-*MoveCustomer* move.

Fig. 4. *Merge* shaking operators

Fig. 4. Alt Text: Figure 4 illustrates the working mechanism of the *Merge* neighborhood operators. The illustrations on the left and on the right show the routes before and after the operator has been applied, respectively. Fig. 4 (a) shows the move where the first route is appended to the end of the second route directly and Fig. 4 (b) depicts the case where the first route is appended to the end of the second route via a recharging station.

Fig. 5. Local search operators

Fig. 5. Alt Text: Figure 5 illustrates the working mechanism of the *Merge* neighborhood operators. The illustrations on the left and on the right show the routes before and after the operator has been applied, respectively. Fig. 5(a) shows *2-Opt* operator that prevents the formation of crisscross arcs in a route and Fig. 5(b) depicts the *2-Opt** operator as an inter-route move adapted from *2-Opt*. Fig. 5(c) presents the *1-AddRecharge* move that inserts a recharging visit in the route and Fig. 5(d) illustrates the *1-DropRecharge* move that removes the recharging visit from the route.

Fig. 6. Visualization of the routes in the current single delivery location setting

Fig. 6. Alt Text: This figure shows the geographical locations of 40 customers selected in the Nottinghamshire, Derbyshire, Lincolnshire, and Loughborough counties and the routes when each has specified a single delivery location. Five vehicles perform the deliveries and two of them recharge en-route. The total distance travelled is 583.22 km.

Fig. 7. The geographical locations of the depot and each customer alternative locations

Fig. 7. Alt Text: This figure shows the alternative delivery points associated with the same 40 customers. 15 customers have two alternative delivery locations, 20 customers have three locations, whereas the remaining five customers still have single delivery location.

Fig. 8. Visualization of the solution obtained by VNS/GTS

Fig. 8. Alt Text: This figure depicts the deliveries to the 40 customers whose flexible delivery points are illustrated in Fig.8. The yellow nodes show the locations where deliveries are made. Four vehicles perform the deliveries and two recharges occur en-route. The total distance travelled is 447.96 km.

Fig. 9. Visualization of the routes for recharging in public stations

Fig. 9. Alt Text: This figure illustrates the solution of the same problem but by allowing vehicles to recharge at available public charging stations. Charger icons indicate the locations of four stations. The yellow nodes show the locations where deliveries are made. Three vehicles perform the deliveries and eight recharges occur en-route. The total distance travelled is 228.73 km.

Acknowledgments

The authors thank the associate editor and four anonymous referees for their valuable comments and suggestions.

Data Availability Statement

The authors confirm that the data supporting the findings of this study are available within the article and the following link: https://sml.sabanciuniv.edu/EVRPFD_Solutions.zip

References

- Abbasi, B., Niaki, S.T.A., Khalife, M.A. and Faize, Y., 2011. A hybrid variable neighborhood search and simulated annealing algorithm to estimate the three parameters of the Weibull distribution. *Expert Systems with Applications*, 38(1), 700–708.
- Andelmin, J. and Bartolini, E., 2017. An exact algorithm for the green vehicle routing problem. *Transportation Science*, 51(4), 1288–1303.
- Aras, N., Aksen, D. and Tekin, M.T., 2011. Selective multi-depot vehicle routing problem with pricing. *Transportation Research Part C: Emerging Technologies*, 19(5), 866–884.
- Baker, R., Cochran, L.K., Norboge, N.D., Moran, M.M., Wagner, J.A., Storey, B.J., 2016. *Alternative Fuel Vehicle Forecasts. Final Report PRC 14-28F*. Transportation Policy Research Center, Texas A&M Transportation Institute.
- Baniamerian, A., Bashiri, M. and Tavakkoli-Moghaddam, R., 2019. Modified variable neighborhood search and genetic algorithm for profitable heterogeneous vehicle routing problem with cross-docking. *Applied Soft Computing*, 75, 441–460.
- BBC. <https://www.bbc.com/news/science-environment-54981425> (last accessed: 06.06.2021).
- BEDEO. <https://bedeo.co.uk> (last accessed: 06.06.2021).
- Beheshti, A.K., Hejazi, S.R., Alinaghian, M., 2015. The vehicle routing problem with multiple prioritized time windows: A case study *Computers & Industrial Engineering*, 90, 402–413.

- Belhaiza, S., Hansen, P. and Laporte, G., 2014. A hybrid variable neighborhood tabu search heuristic for the vehicle routing problem with multiple time windows. *Computers & Operations Research*, 52, 269–281.
- Bortfeldt, A., Hahn, T., Männel, D. and Mönch, L., 2015. Hybrid algorithms for the vehicle routing problem with clustered backhauls and 3D loading constraints. *European Journal of Operational Research*, 243(1), 82–96.
- Bruglieri, M., Mancini, S., Pezzella, F. and Pisacane, O., 2016. A new mathematical programming model for the green vehicle routing problem. *Electronic Notes in Discrete Mathematics*, 55, 89–92.
- Bruglieri, M., Mancini, S., Pezzella, F. and Pisacane, O., 2019. A path-based solution approach for the green vehicle routing problem. *Computers & Operations Research*, 103, 109–122.
- Bruglieri, M., Pezzella, F., Pisacane, O., Suraci, S., 2015. A variable neighborhood search branching for the electric vehicle routing problem with time windows. *Electron. Notes Discret. Math.* 47, 221–228.
- Bubner, N., Bubner, N., Helbig, R. and Jeske, M., 2013. Logistics trend radar. Delivering insight today. Creating value tomorrow. DHL Customer Solutions & Innovation, Troisdorf, Germany. Available at: https://www.dhl.com/content/dam/Campaigns/InnovationDay_2013/90310673_HI-RES.PDF (last accessed: 06.06.2021)
- Business Insider. <https://www.businessinsider.com/amazon-creating-fleet-of-electric-delivery-vehicles-rivian-2020-2> (last accessed: 06.06.2021).
- Coelho, I.M., Munhoz, P.L.A., Ochi, L.S., Souza, M.J.F., Bentes, C. and Farias, R., 2016. An integrated CPU–GPU heuristic inspired on variable neighbourhood search for the single vehicle routing problem with deliveries and selective pickups. *International Journal of Production Research*, 54(4), 945–962.
- Chagas, J.B., Silveira, U.E., Santos, A.G. and Souza, M.J., 2020. A variable neighborhood search heuristic algorithm for the double vehicle routing problem with multiple stacks. *International Transactions in Operational Research*, 27(1), 112–137.

- Conrad, R.G., Figliozzi, M.A., 2011. The recharging vehicle routing problem. In: Doolen, T. and Van Aken, E. (eds) Proceedings of the 2011 Industrial Engineering Research Conference. Reno, NV, 2011.
- Cordeau, J.F., Gendreau, M. and Laporte, G., 1997. A tabu search heuristic for periodic and multi-depot vehicle routing problems. *Networks: An International Journal*, 30(2), 105–119.
- Cortés-Murcia, D.L., Prodhon, C. and Afsar, H.M., 2019. The electric vehicle routing problem with time windows, partial recharges and satellite customers. *Transportation Research Part E: Logistics and Transportation Review*, 130, 184–206.
- de Jong, C., Kant, G., van Vliet, A., 1996. On finding minimal route duration in the vehicle routing problem with multiple time windows. Manuscript, Department of Computer Science, Utrecht University, Netherlands.
- Desaulniers, G., Errico, F., Irnich, S. and Schneider, M., 2016. Exact algorithms for electric vehicle routing problems with time windows. *Operations Research*, 64(6), 1388–1405.
- Doerner K.F., Gronalt M., Hartl R.F., Kiechle, G., Reimann, M., 2008. Exact and heuristic algorithms for the vehicle routing problem with multiple interdependent time windows. *Computers & Operations Research*, 35(9), 3034–3048.
- Duman, E.N., Taş, D. and Çatay, B., 2021. Branch-and-price-and-cut methods for the electric vehicle routing problem with time windows. *International Journal of Production Research*, 1-22 (published online).
- Elshaer, R. and Awad, H., 2020. A taxonomic review of metaheuristic algorithms for solving the vehicle routing problem and its variants. *Computers & Industrial Engineering*, 140, p.106242.
- Erdelić, T., Carić, T., 2019. A survey on the electric vehicle routing problem: variants and solution approaches. *Journal of Advanced Transportation* 2019, 5075671.
- Erdoğan, G., 2017. An open source spreadsheet solver for vehicle routing problems. *Computers & Operations Research*, 84, 62–72
- Erdoğan, S. and Miller-Hooks, E., 2012. A green vehicle routing problem. *Transportation Research Part E: Logistics and Transportation Review*, 48(1), 100–114.

- European Commission, 2013. Urban Mobility Package: Together Towards Competitive and Resource Efficient Urban Mobility. https://ec.europa.eu/transport/themes/urban/urban-mobility/urban-mobility-package_en (last accessed: 06.06.2021).
- Felipe, Á., Ortuño, M.T., Righini, G. and Tirado, G., 2014. A heuristic approach for the green vehicle routing problem with multiple technologies and partial recharges. *Transportation Research Part E: Logistics and Transportation Review*, 71, 111–128.
- Favaretto D., Moretti E., Pellegrini P., 2007. Ant colony system for a VRP with multiple time windows and multiple visits. *Journal of Interdisciplinary Mathematics*, 10, 263–84.
- Froger, A., Mendoza, J.E., Jabali, O. and Laporte, G., 2019. Improved formulations and algorithmic components for the electric vehicle routing problem with nonlinear charging functions. *Computers & Operations Research*, 104, 256–294.
- FUELSAVE. <https://fuelsave-global.com/which-country-will-become-the-first-to-ban-internal-combustion-cars/> (last accessed: 06.06.2021).
- Gendreau, M., Iori, M., Laporte, G. and Martello, S., 2008. A tabu search heuristic for the vehicle routing problem with two-dimensional loading constraints. *Networks: An International Journal*, 51(1), 4–18.
- Ghiani, G., & Improta, G., 2000. An efficient transformation of the generalized vehicle routing problem. *European Journal of Operational Research*, 122(1), 11-17.
- Giordano, A., Fischbeck, P. and Matthews, H.S., 2018. Environmental and economic comparison of diesel and battery electric delivery vans to inform city logistics fleet replacement strategies. *Transportation Research Part D: Transport and Environment*, 64, 216–229.
- Goeke, D. and Schneider, M., 2015. Routing a mixed fleet of electric and conventional vehicles. *European Journal of Operational Research*, 245(1), 81–99.
- Hiermann, G., Puchinger, J., Ropke, S. and Hartl, R.F., 2016. The electric fleet size and mix vehicle routing problem with time windows and recharging stations. *European Journal of Operational Research*, 252(3), 995–1018.

- Hiermann, G., Hartl, R.F., Puchinger, J. and Vidal, T., 2019. Routing a mix of conventional, plug-in hybrid, and electric vehicles. *European Journal of Operational Research*, 272(1), 235–248.
- Hintsch, T. and Irnich, S., 2018. Large multiple neighborhood search for the clustered vehicle-routing problem. *European Journal of Operational Research*, 270(1), 118–131.
- Hirsch, P. and Gronalt, M., 2007. Tabu search based solution methods for scheduling log-trucks. TRISTAN VI-The Sixth Triennial Symposium on Transportation Analysis, Phuket, Thailand.
- Hof, J., Schneider, M. and Goeke, D., 2017. Solving the battery swap station location-routing problem with capacitated electric vehicles using an AVNS algorithm for vehicle-routing problems with intermediate stops. *Transportation Research Part B: Methodological*, 97, 102–112.
- Hosseini, S., Al Khaled, A. and Vadlamani, S., 2014. Hybrid imperialist competitive algorithm, variable neighborhood search, and simulated annealing for dynamic facility layout problem. *Neural Computing and Applications*, 25(7-8), 1871–1885.
- Jaller, M., Pineda, L. and Ambrose, H., 2018. Evaluating the use of zero-emission vehicles in last mile deliveries. Institute of Transportation Studies, University of California, Davis, Research Report UCD-ITS-RR-18-48.
- Jie, W., Yang, J., Zhang, M. and Huang, Y., 2019. The two-echelon capacitated electric vehicle routing problem with battery swapping stations: Formulation and efficient methodology. *European Journal of Operational Research*, 272(3), 879–904.
- Kancharla, S.R. and Ramadurai, G., 2020. Electric vehicle routing problem with non-linear charging and load-dependent discharging. *Expert Systems with Applications*, 160, 113714.
- Keskin, M. and Çatay, B., 2016. Partial recharge strategies for the electric vehicle routing problem with time windows. *Transportation Research Part C: Emerging Technologies*, 65, 111–127.
- Keskin, M. and Çatay, B., 2018. A matheuristic method for the electric vehicle routing problem with time windows and fast chargers. *Computers & Operations Research*, 100, 172–188.
- Keskin, M., Laporte, G. and Çatay, B., 2019. Electric vehicle routing problem with time-dependent waiting times at recharging stations. *Computers & Operations Research*, 107, 77–94.

- Keskin, M., Çatay, B. and Laporte, G., 2021. A simulation-based heuristic for the electric vehicle routing problem with time windows and stochastic waiting times at recharging stations. *Computers & Operations Research*, 125, 105060.
- Kullman, N., Goodson, J. and Mendoza, J.E., 2021. Electric vehicle routing with public charging stations. *Transportation Science*, 55(3), 637–659.
- Lewis, M., Hearn, C., Feng, X., Hanlin, J., Levin, J., Ambrosio, J., Guggenheim, P. and Walker, C., 2017. Design and modeling for hydrogen fuel cell conversion of parcel delivery trucks. 2017 IEEE Transportation Electrification Conference and Expo (ITEC), Chicago, IL, 674–678.
- Li, X., Gao, L., Pan, Q., Wan, L. and Chao, K.M., 2018. An effective hybrid genetic algorithm and variable neighborhood search for integrated process planning and scheduling in a packaging machine workshop. *IEEE Transactions on Systems, Man, and Cybernetics: Systems*, 49(10), 1933–1945.
- Macrina, G., Pugliese, L.D.P., Guerriero, F. and Laporte, G., 2019. The green mixed fleet vehicle routing problem with partial battery recharging and time windows. *Computers & Operations Research*, 101, 183–199.
- Mancini, S., 2017. The hybrid vehicle routing problem. *Transportation Research Part C: Emerging Technologies*, 78, 1–12.
- Marinakis, Y., Migdalas, A. and Sifaleras, A., 2017. A hybrid particle swarm optimization–variable neighborhood search algorithm for constrained shortest path problems. *European Journal of Operational Research*, 261(3), 819–834.
- Masmoudi, M.A., Hosny, M., Demir, E., Genikomsakis, K.N. and Cheikhrouhou, N., 2018. The dial-a-ride problem with electric vehicles and battery swapping stations. *Transportation Research Part E: Logistics and Transportation Review*, 118, 392–420.
- Mitreă, I.A., 2020. Estimating e-commerce demand for last mile delivery optimization through parcel locker. Unpublished Master's Thesis, Politecnico di Torino. Available at: <https://webthesis.biblio.polito.it/14704/>

- Mladenović, N. and Hansen, P., 1997. Variable neighborhood search. *Computers & Operations Research*, 24(11), 1097–1100.
- Montoya, A., Guéret, C., Mendoza, J.E., Villegas, J.G., 2016. A multi-space sampling heuristic for the green vehicle routing problem. *Transportation Research Part E: Logistics and Transportation Review*, 70, 113–128.
- Montoya, A., Guéret, C., Mendoza, J.E. and Villegas, J.G., 2017. The electric vehicle routing problem with nonlinear charging function. *Transportation Research Part B: Methodological*, 103, 87–110.
- Morganti, E., Browne, M., 2018. Technical and operational obstacles to the adoption of electric vans in France and the UK: An operator perspective. *Transport Policy*, 63, 90–97.
- Ozbaygin, G., Karasan, O.E., Savelsbergh, M. and Yaman, H., 2017. A branch-and-price algorithm for the vehicle routing problem with roaming delivery locations. *Transportation Research Part B: Methodological*, 100, 115–137.
- Ozbaygin, G. and Savelsbergh, M., 2019. An iterative re-optimization framework for the dynamic vehicle routing problem with roaming delivery locations. *Transportation Research Part B: Methodological*, 128, 207–235.
- Pan, S., Zhang, L., Thompson, R.G. and Ghaderi, H., 2021a. A parcel network flow approach for joint delivery networks using parcel lockers. *International Journal of Production Research*, 59(7), 2090–2115.
- Pan, S., Zhou, W., Piramuthu, S., Giannikas, V. and Chen, C., 2021b. Smart city for sustainable urban freight logistics. *International Journal of Production Research*, 59(7), 2079–2089.
- Paydar, M.M. and Saidi-Mehrabad, M., 2013. A hybrid genetic-variable neighborhood search algorithm for the cell formation problem based on grouping efficacy. *Computers & Operations Research*, 40(4), 980–990.
- Pelletier, S., Jabali, O., Laporte, G. and Veneroni, M., 2017. Battery degradation and behaviour for electric vehicles: Review and numerical analyses of several models. *Transportation Research Part B: Methodological*, 103, 158–187.

- Potvin, J.Y. and Rousseau, J.M., 1995. An exchange heuristic for routing problems with time windows. *Journal of the Operational Research Society*, 46(12), 1433–1446.
- Prandtstetter, M. and Raidl, G.R., 2008. An integer linear programming approach and a hybrid variable neighborhood search for the car sequencing problem. *European Journal of Operational Research*, 191(3), 1004–1022.
- Rastani, S., Yüksel, T. and Çatay, B., 2019. Effects of ambient temperature on the route planning of electric freight vehicles. *Transportation Research Part D: Transport and Environment*, 74, 124–141.
- Rastani, S., Yüksel, T. and Çatay, B., 2020. Electric vehicle routing problem with time windows and cargo weight. In: Golinska-Dawson P., Tsai KM., Kosacka-Olejnik M. (eds.), *Smart and Sustainable Supply Chain and Logistics – Trends, Challenges, Methods and Best Practices. EcoProduction (Environmental Issues in Logistics and Manufacturing)*, Switzerland:175–190.
- Rastani, S. and Çatay, B., 2021. A large neighborhood search-based matheuristic for the load-dependent electric vehicle routing problem with time windows. *Annals of Operations Research*, 1-33.
- Reuters. <https://www.reuters.com/article/us-usa-biden-autos-idUSKBN29U2LW> (last accessed: 06.06.2021).
- Reyes, D., Savelsbergh, M. and Toriello, A., 2017. Vehicle routing with roaming delivery locations. *Transportation Research Part C: Emerging Technologies*, 80, 71–91.
- Rezgui, D., Siala, J.C., Aggoune-Mtalaa, W. and Bouziri, H., 2019. Application of a variable neighborhood search algorithm to a fleet size and mix vehicle routing problem with electric modular vehicles. *Computers & Industrial Engineering*, 130, 537–550.
- Sadati, M.E.H., Aksen, D. and Aras, N., 2020. A trilevel r-interdiction selective multi-depot vehicle routing problem with depot protection. *Computers & operations research*, 123, 104996.
- Sadati, M.E.H., Çatay, B. and Aksen, D., 2021. An efficient variable neighborhood search with tabu shaking for a class of multi-depot vehicle routing problems. *Computers & Operations Research*, 133, 105269.

- Sadati, M.E.H. and Çatay, B., 2021. A hybrid variable neighborhood search approach for the multi-depot green vehicle routing problem. *Transportation Research Part E: Logistics and Transportation Review*, 149, 102293.
- Sassi, O. and Oulamara, A., 2017. Electric vehicle scheduling and optimal charging problem: complexity, exact and heuristic approaches. *International Journal of Production Research*, 55(2), 519–535.
- Schermer, D., Moeini, M. and Wendt, O., 2019. A hybrid VNS/Tabu search algorithm for solving the vehicle routing problem with drones and en route operations. *Computers & Operations Research*, 109, 134–158.
- Schneider, M., Stenger, A. and Goeke, D., 2014. The electric vehicle routing problem with time windows and recharging stations. *Transportation Science*, 48(4), 500–520.
- Schneider, M., Stenger, A., Hof, J., 2015. An adaptive VNS algorithm for vehicle routing problems with intermediate stops. *OR Spectrum*, 37, 353–387.
- Sweda, T.M., Dolinskaya, I.S. and Klabjan, D., 2017. Adaptive routing and recharging policies for electric vehicles. *Transportation Science*, 51(4), 1326–1348.
- Tilk, C., Olkis, K. & Irnich, S. The last-mile vehicle routing problem with delivery options. *OR Spectrum* (2021). <https://doi.org/10.1007/s00291-021-00633-0>
- Ting, T.O., Yang, X.S., Cheng, S. and Huang, K., 2015. Hybrid metaheuristic algorithms: past, present, and future. In: *Recent advances in swarm intelligence and evolutionary computation* (71–83). Springer, Cham.
- Toth, P. and Vigo, D., 2003. The granular tabu search and its application to the vehicle routing problem. *Inform Journal on Computing*, 15(4), 333–346.
- United Nations Conference on Trade and Development. <https://unctad.org/news/covid-19-has-changed-online-shopping-forever-survey-shows> (last accessed: 06.06.2021).
- UPS. <https://www.ups.com/us/en/services/e-commerce/access-point-network.page?> (Last accessed: 06.06.2021)

- Wang, Y.W., Lin, C.C. and Lee, T.J., 2018. Electric vehicle tour planning. *Transportation Research Part D: Transport and Environment*, 63, 121–136.
- Wei, L., Zhang, Z., Zhang, D. and Lim, A., 2015. A variable neighborhood search for the capacitated vehicle routing problem with two-dimensional loading constraints. *European Journal of Operational Research*, 243(3), 798–814.
- Xia, H., Li, X. and Gao, L., 2016. A hybrid genetic algorithm with variable neighborhood search for dynamic integrated process planning and scheduling. *Computers & Industrial Engineering*, 102, 99–112.
- Yang, J. and Sun, H., 2015. Battery swap station location-routing problem with capacitated electric vehicles. *Computers & Operations Research*, 55, 217–232.
- Zhen, L., Xu, Z., Ma, C. and Xiao, L., 2020. Hybrid electric vehicle routing problem with mode selection. *International Journal of Production Research*, 58(2), 562–576.F

Appendix A

Table A.1 and Table A.2 present the results for the first and second set of VRPRDL instances, respectively, in comparison with the optimal solutions obtained by the branch-price-and-cut algorithm of Tilk et al. (2021).

Table A.1. Results of the first set of VRPRDL instances

Instance	n	Optimal	VNS/GTS			
			Best	Avg	Best $\Delta\%$	Avg $\Delta\%$
1	15	901	901	901	0.00	0.00
2	15	1286	1286	1286	0.00	0.00
3	15	991	991	991	0.00	0.00
4	15	1062	1062	1062	0.00	0.00
5	15	1832	1832	1832	0.00	0.00
6	20	1294	1294	1294	0.00	0.00
7	20	1155	1155	1155	0.00	0.00
8	20	1455	1455	1455	0.00	0.00
9	20	1260	1260	1260	0.00	0.00
10	20	1684	1684	1684	0.00	0.00
11	30	1922	1922	1923	0.00	0.05
12	30	2324	2324	2326	0.00	0.09
13	30	1747	1747	1751	0.00	0.23
14	30	1273	1273	1275	0.00	0.16
15	30	1694	1694	1697	0.00	0.18
16	30	1938	1938	1939	0.00	0.05
17	30	1965	1965	1967	0.00	0.10
18	30	1827	1827	1827	0.00	0.00
19	30	2083	2083	2083	0.00	0.00
20	30	1822	1822	1822	0.00	0.00
21	60	3761	3765	3768	0.11	0.19
22	60	2828	2828	2835	0.00	0.25
23	60	4440	4445	4449	0.11	0.20
24	60	3378	3381	3385	0.09	0.21
25	60	3161	3166	3168	0.16	0.22
26	60	4536	4536	4537	0.00	0.02
27	60	2865	2870	2874	0.17	0.31
28	60	4173	4176	4183	0.07	0.24
29	60	3964	3966	3970	0.05	0.15
30	60	4107	4115	4118	0.19	0.27
31	120	4935	4940	4941	0.10	0.12
32	120	5258	5290	5292	0.61	0.65
33	120	5061	5098	5102	0.73	0.81
34	120	5218	5230	5237	0.23	0.36
35	120	5498	5545	5548	0.85	0.91
36	120	6498	6498	6502	0.00	0.06
37	120	4830	4863	4867	0.68	0.77
38	120	5604	5619	5620	0.27	0.29
39	120	5841	5890	5892	0.84	0.87
40	120	4995	5057	5059	1.24	1.28
Average		3061.65	3069.83	3071.93	0.16	0.23

Table A.2. Results of the second set of VRPRDL instances

Instance	n	Optimal	VNS/GTS			
			Best	Avg	Best $\Delta\%$	Avg $\Delta\%$
41_v1	40	3203	3203	3204	0.00	0.03
41_v2	40	2133	2135	2136	0.09	0.14
42_v1	40	2799	2801	2802	0.07	0.11
42_v2	40	1946	1946	1948	0.00	0.10
43_v1	40	2603	2615	2617	0.46	0.54
43_v2	40	1966	1969	1971	0.15	0.25
44_v1	40	2261	2261	2262	0.00	0.04
44_v2	40	1610	1610	1613	0.00	0.19
45_v1	40	3217	3217	3219	0.00	0.06
45_v2	40	2478	2482	2483	0.16	0.20
46_v1	40	2805	2805	2806	0.00	0.04
46_v2	40	2469	2469	2471	0.00	0.08
47_v1	40	3339	3339	3341	0.00	0.06
47_v2	40	1946	1946	1949	0.00	0.15
48_v1	40	3325	3330	3332	0.15	0.21
48_v2	40	2380	2380	2381	0.00	0.04
49_v1	40	3534	3534	3536	0.00	0.06
49_v2	40	2492	2498	2499	0.24	0.28
50_v1	40	2752	2759	2762	0.25	0.36
50_v2	40	2443	2448	2450	0.20	0.29
Average		2585.05	2587.35	2589.10	0.09	0.16

Appendix B

Table B.1 through Table B.3 present the detailed information of customers and associated delivery locations used in the case study.

Table B.1. Customer data

Customer	Demand	Latitude	Longitude	TW
1	2	53.00217	-1.28443	2PM-6PM
2	5	52.93966	-1.20719	7AM-1PM
3	4	52.95683	-1.19696	2PM-6PM
4	2	53.00071	-1.13181	7AM-1PM
5	2	52.97144	-1.36236	7PM-11PM
6	5	53.09691	-1.38011	2PM-6PM
7	2	53.19792	-1.39174	7AM-1PM
8	3	52.97007	-1.45786	7PM-11PM
9	4	52.91285	-0.98748	2PM-6PM
10	3	53.05171	-1.40624	7PM-11PM
11	3	52.92782	-1.27492	7AM-1PM
12	3	52.92950	-1.29232	2PM-6PM
13	4	52.92907	-1.22245	2PM-6PM
14	5	52.90512	-1.25272	7AM-1PM
15	5	52.96221	-1.07466	7PM-11PM
16	1	52.91985	-1.48703	7AM-1PM
17	4	53.07783	-0.95281	7PM-11PM
18	4	52.92532	-1.53483	2PM-6PM
19	4	53.01919	-1.62114	7PM-11PM
20	3	52.92687	-1.54442	2PM-6PM
21	1	52.90039	-1.51959	7AM-1PM
22	2	53.02310	-1.06359	2PM-6PM
23	3	52.94808	-0.94328	7PM-11PM
24	1	53.10341	-1.25540	7AM-1PM
25	5	53.10557	-1.33819	7PM-11PM
26	2	53.11378	-1.11791	2PM-6PM
27	3	52.97139	-1.09135	7AM-1PM
28	5	53.04797	-1.60254	2PM-6PM
29	5	52.96988	-1.62356	7PM-11PM
30	5	52.77941	-1.20671	7AM-1PM
31	5	52.82086	-1.25072	7AM-1PM
32	3	52.98331	-0.96556	2PM-6PM
33	4	52.81182	-1.47493	2PM-6PM
34	4	53.02537	-1.17932	2PM-6PM
35	2	52.92770	-1.10285	7AM-1PM
36	4	52.83094	-1.14577	7PM-11PM
37	3	52.78149	-1.33862	2PM-6PM
38	3	52.94957	-1.03587	7AM-1PM
39	5	53.16337	-1.41609	2PM-6PM
40	4	53.17125	-1.25040	7AM-1PM

Table B.2. Location information in flexible delivery options

Customer	Location 1		Location 2				Location 3			
	ID	TW	ID	Latitude	Longitude	TW	ID	Latitude	Longitude	TW
1	1	3PM-6PM	41	53.09626	-1.22699	9AM-12PM	76	52.80929	-1.10600	6PM-9PM
2	2	9AM-12PM								
3	3	3PM-6PM	42	53.03011	-1.44171	6PM-9PM	77	52.97107	-0.90326	12PM-3PM
4	4	9AM-12PM	43	53.08121	-0.91852	12PM-3PM	78	53.10935	-1.12126	6PM-9PM
5	5	6PM-9PM								
6	6	3PM-6PM	44	53.05894	-1.05586	6PM-9PM				
7	7	9AM-12PM	45	52.83564	-1.12453	12PM-3PM	79	52.96269	-1.15291	3PM-6PM
8	8	6PM-9PM	46	53.08383	-1.48204	3PM-6PM	80	53.04191	-0.95885	12PM-3PM
9	9	12PM-3PM								
10	10	6PM-9PM	47	52.81720	-1.23571	9AM-12PM				
11	11	12PM-3PM	48	53.12089	-1.10063	6PM-9PM	81	52.83804	-1.10390	3PM-6PM
12	12	3PM-6PM	49	52.86700	-1.20745	12PM-3PM	82	52.85318	-1.42980	9AM-12PM
13	13	12PM-3PM								
14	14	9AM-12PM	50	53.01414	-1.41563	3PM-6PM				
15	15	6PM-9PM	51	53.13920	-1.36658	9AM-12PM	83	53.13659	-0.86192	3PM-6PM
16	16	12PM-3PM	52	52.87752	-0.99272	3PM-6PM	84	53.00692	-0.82704	6PM-9PM
17	17	6PM-9PM	53	52.95573	-1.34151	12PM-3PM				
18	18	3PM-6PM	54	53.13986	-1.19873	12PM-3PM	85	52.88936	-0.84884	9AM-12PM
19	19	6PM-9PM	55	53.05936	-1.40255	9AM-12PM	86	53.11566	-0.86410	3PM-6PM
20	20	12PM-3PM	56	53.09210	-1.45705	6PM-9PM				
21	21	9AM-12PM	57	53.13855	-0.93168	12PM-3PM	87	52.82618	-0.74856	6PM-9PM
22	22	3PM-6PM	58	53.11500	-1.49520	6PM-9PM				
23	23	6PM-9PM	59	52.90712	-0.94585	3PM-6PM				
24	24	9AM-12PM	60	53.08817	-1.48212	3PM-6PM	88	52.87884	-1.41345	6PM-9PM
25	25	6PM-9PM	61	52.81564	-1.22925	3PM-6PM				
26	26	3PM-6PM	62	52.84989	-1.40582	9AM-12PM	89	53.12416	-1.12897	12PM-3PM
27	27	12PM-3PM	63	53.11762	-1.49738	3PM-6PM				
28	28	3PM-6PM	64	52.97871	-0.80742	12PM-3PM	90	53.09603	-1.14641	9AM-12PM
29	29	6PM-9PM	65	52.81235	-1.24124	3PM-6PM				
30	30	9AM-12PM								
31	31	12PM-3PM	66	52.89660	-1.39492	9AM-12PM	91	52.87752	-0.79543	6PM-9PM
32	32	3PM-6PM	67	53.06001	-1.37530	9AM-12PM				
33	33	3PM-6PM	68	52.80444	-1.27721	6PM-9PM				
34	34	12PM-3PM	69	53.11304	-1.24887	3PM-6PM	92	52.98724	-1.57150	9AM-12PM
35	35	9AM-12PM	70	52.82948	-1.36113	6PM-9PM				
36	36	6PM-9PM	71	52.78731	-1.01779	12PM-3PM	93	53.14770	-0.94367	3PM-6PM
37	37	3PM-6PM	72	53.08686	-1.46468	6PM-9PM				
38	38	9AM-12PM	73	53.14247	-1.04722	12PM-3PM	94	52.94063	-1.43525	3PM-6PM
39	39	12PM-3PM	74	53.03643	-1.57259	6PM-9PM				
40	40	9AM-12PM	75	53.05870	-0.88808	6PM-9PM	95	53.09341	-1.65870	12PM-3PM

Table B.3. Public station locations

Station	Latitude	Longitude
S1	52.9891175	-0.9780477
S2	53.1354618	-1.2249143
S3	53.0210944	-1.4870107
S4	52.9047598	-1.4251326

Appendix C

Table C.1 presents the detailed route plans in the case study under different settings. In this table “D”, “R” and “S” denotes the depot, recharge en-route (recharging at depot), and public station, respectively. The last column reports the return time of the vehicle to the depot at the end of its tour.

Table C.1. Route plans in the case study under different settings

Current Setting:

EV	Delivery Route	Distance	Return Time
1	D, 27, 35, 38, 9, 32, 23, 17, 15, D	99.09	10:36 PM
2	D, 31, 30, 36, D	67.26	9:44 PM
3	D, 2, 14, 11, 16, 21, 20, 18, 12, 13, 3, R, 1, 28, 19, 29, 8, 5, D	187.79	10:41 PM
4	D, 4, 22, 26, 34, R, 37, 33, D	134.61	8:22 PM
5	D, 24, 40, 7, 39, 6, 25, 10, D	94.47	10:00 PM
Total		583.22	

Flexible Deliveries:

EV	Delivery Route	Distance	Return Time
1	D, 30, 31, 49, 13, R, 34, 79, 3, R, 26, 93, 86, 75, 17, 44, D	173.11	7:58 PM
2	D, 4, 35, 38, 9, 59, 52, 81, 61, 65, 68, D	99.64	8:00 PM
3	D, 2, 14, 21, 18, 8, 5, D	79.79	7:54 PM
4	D, 90, 41, 24, 67, 51, 39, 63, 58, 72, 56, D	95.42	8:40 PM
Total		447.96	

Flexible Deliveries using Public Charging:

EV	Delivery Route	Distance	Return Time
1	D, 62, 82, S4, 38, 9, 52, 59, 32, S1, 79, 3, R, 6, 56, 63, 58, 46, 72, S3, D	92.58	8:50 PM
2	D, 4, 2, 13, 14, 11, 53, S4, 34, 54, 57, 93, 83, 86, 75, R, 28, 74, D	72.64	8:45 PM
3	D, 41, S2, 24, 30, 47, 31, 65, 61, 68, 70, S4, 5, D	63.51	8:20 PM
Total		228.73	